

Time Matters in Using Data Augmentation for Vision-Based Deep Reinforcement Learning

Byungchan Ko¹ Jungseul Ok^{1,2}

Abstract

Data augmentation technique from computer vision has been widely considered as a regularization method to improve data efficiency and generalization performance in vision-based reinforcement learning. We variate the timing of using augmentation, which is, in turn, critical depending on tasks to be solved in training and testing. According to our experiments on Open AI Procgen Benchmark, if the regularization imposed by augmentation is helpful only in testing, it is better to procrastinate the augmentation after training than to use it during training in terms of sample and computation complexity. We note that some of such augmentations can disturb the training process. Conversely, an augmentation providing regularization useful in training needs to be used during the whole training period to fully utilize its benefit in terms of not only generalization but also data efficiency. These phenomena suggest a useful timing control of data augmentation in reinforcement learning.

1. Introduction

Reinforcement Learning (RL) from visual observations is a fundamental problem since visual data is one of the most common observations available in practice, e.g., video game (Mnih et al., 2015), board game (Silver et al., 2017; 2018), and robot (Tobin et al., 2017; Kalashnikov et al., 2018). However, such a vision-based RL often suffers from the problem of sample efficiency and generalization capability due to the high-dimensional nature of images. As a part of overcoming this, regularization by data augmentation has been widely considered (Laskin et al., 2020; Kostrikov et al., 2020), where visual data is augmented by transformation preserving the same meaning or context, e.g., cropping out

unimportant part of images or randomizing backgrounds. It not only resolves the data scarcity but also provides an explicit implementation of inductive bias for generalization performance.

Recent works show that using the right types of data augmentation significantly improves both data efficiency and generalization performance (Raileanu et al., 2020). However, choosing the right data augmentation is found to be highly task-dependent, where poor choice can degenerate the generalization and destabilize the training (Laskin et al., 2020; Raileanu et al., 2020). Hence, a variety of transformations have been developed to enlarge the set of data augmentation (Lee et al., 2019; Hansen & Wang, 2020). A number of regularization methods using data augmentation, meanwhile, have been proposed to stabilize training process with data augmentation, e.g., self-supervised learning (Raileanu et al., 2020) and representation learning (Srinivas et al., 2020; Hansen & Wang, 2020) by reducing the interference between RL training and regularization. Although the previous works address *what* data augmentation to use and *how* to use it, but the understanding on *when* to apply it in the training process is limited. We test the hypothesis that applying augmentation method at different epochs can have different effects. This is a non-trivial question since the timing of data augmentation is not critical in supervised learning (SL) (Achille et al., 2018; Golatkar et al., 2019), whereas a curriculum learning can accelerate RL training (Raparthi et al., 2020).

To address our main question, we devise two frameworks with different timings of applying augmentation: InDA (Intra Distillation with Augmented observations) and ExDA (Extra Distillation with Augmented observations) (Section 3). Implementing the regularization via augmentation in a form of distillation to minimize interference in RL training, InDA interleave the distillation with RL training, while ExDA applies the distillation at the end of RL training. From experiments with InDA and ExDA, we find that:

Time does matter when using augmentation in RL

in contrast to the case of SL (Golatkar et al., 2019) where the effect of data augmentation is relatively insensitive to timing. The difference mainly comes from the fact that RL

¹Graduate School of Artificial Intelligence, POSTECH, Pohang, Korea ²Department of Computer Science and Engineering, POSTECH, Pohang, Korea. Correspondence to: Jungseul Ok <jungseul@postech.ac.kr>.

agent collects samples when training but SL uses a fixed data set. To be specific, our main findings from experiments are given in two folds:

- (i) Applying augmentation *needs* to be applied as *early* as possible for sample efficiency and generalization if it can accelerate RL training, e.g., cropping out unnecessary part of image induces an efficient attention mechanism. It is obvious that we need to accelerate RL training from beginning in order to maximize sample efficiency. However, interestingly, we observe that this kind of augmentation often connotes generalization which is transferable only through diverse experience in training process, i.e., ExDA does not fully exploit generalization gain whereas InDA does. Hence, it is indeed necessary to use such an augmentation during training to gain generalization. (Section 4.1)
- (ii) Applying augmentation *needs* to be *postponed to the end* of RL training for sample efficiency if the regularization imposed by augmentation is helpful only in testing, e.g., augmentation by changing colors is useless when a single background is shown in training, but testing task has multiple backgrounds. We find that this type of augmentation possibly interferes with RL training but there is no harm in generalization from delaying it. Hence, in this case, ExDA, which never disturbs RL training, is better than InDA. (Section 4.2)

In the above findings, we characterize and suggest effective timings of applying augmentation in RL. In addition to this, our contribution can include proposing InDA and ExDA algorithms, in particular, which is equipped with the distillation augmentation (DA) since it is of independent interest that developing a regularization method using augmentation with minimal interference with RL training. Compared to existing methods DrAC (Raileanu et al., 2020), RAD (Laskin et al., 2020), Rand-FM (Lee et al., 2019), a potential advantage of the proposed one is discussed in Section 3.

2. Related Works

Augmented experience in RL. In order to resolve the problem of poor generalization and sparse data, it is a popular approach to generate diverse (virtual) experiences and let RL agent learn from them. Domain randomization is a technique to produce such experiences from a simulator of targeted system (Tobin et al., 2017; Pinto et al., 2017; Raparthy et al., 2020). It is hard to obtain an accurate simulator of practical systems and thus this limits the spectrum of application. Visual augmentation, meanwhile, has no such limit since it is based on simple image transformations such as cropping, tilting, color jitters and so on, although we need a careful understanding on the targeted system to design appropriate image transformer. Raparthy et al. (2020) propose

a curriculum learning for domain randomization where the difficulty is gradually increasing and the insight coincides with some of our findings. However, we provide further understandings on which types of visual augmentation need to be used as sooner or later as possible.

The regularization from augmented data in vision-based RL has been implemented in various learning frameworks, including but not limited to representation (Hansen & Wang, 2020; Stooke et al., 2020), self-supervised (Raileanu et al., 2020), and contrast (Srinivas et al., 2020). Raileanu et al. (2020) further proposes an algorithm to automatically select the most effective augmentations over RL training based on UCB (Upper Confidence Bound) algorithm (Auer, 2002), where each augmentation is considered as an arm and is evaluated its effectiveness in sliding window. The idea of adapting augmentation shares with our main message regarding the timing of augmentation. In Raileanu et al. (2020), not augmenting is not counted as an arm, while according to our findings, it needs to be. In addition, the post augmentation followed by RL training of ExDA is not considered.

Different time-sensitivity of augmentation than SL. In deep learning, we often observe that the early state of training impacts significantly (Erhan et al., 2010; Achille et al., 2018). Hence, this motivates us to devise time-sensitive methods adapting to the progress of training such as learning rate decay (You et al., 2019) and curriculum learning (Wu et al., 2020). Golatkar et al. (2019) studied such a time-sensitivity of regularization techniques for SL, where the effect of data augmentation in different time does not change much. We find that the time-sensitivity of augmentation can be significant in RL. This contrast perhaps is because of the non-stationary nature of RL, which SL does not have. Although a set of techniques originally developed for SL such as convolutional neural network, weight decay, batch normalization, dropout and self-supervised learning improve deep RL (Higgins et al., 2018; Cobbe et al., 2019; Liu et al., 2020; Farebrother et al., 2020; Srinivas et al., 2020; Yarats et al., 2020; Hansen et al., 2020), a thorough study needs to be in advance of introducing method from different learning framework as we find the contrasting time-sensitivities of data augmentation. This spirit is also shared with an application (Igl et al., 2020) of implicit bias in SL (Gunasekar et al., 2017; Arora et al., 2019; Gidel et al., 2019) to RL.

3. Method

Notation. We consider a standard agent-environment interface of *vision-based* reinforcement learning in discrete Markov decision process of state space \mathcal{S} , action space \mathcal{A} and kernel $P = P(s_{t+1}, r_t | s_t, a_t)$ which determines the state transition and reward distribution. The goal of RL agent is to find policy maximizing the expectation of cumu-

lative reward $\sum_{t=0}^{t'-1} \gamma^t r_t$, where t' is terminating time and $\gamma \in [0, 1]$ is discount factor. At each timestep t , the agent selects an action $a_t \in \mathcal{A}$ and receives reward r_t and an image $o_{t+1} = O(s_{t+1}) \in \mathbb{R}^{k \times k}$ as an (possibly partial) observation of the next state s_{t+1} . To augment observations, we consider image transformation function $\phi : \mathbb{R}^{k \times k} \mapsto \mathbb{R}^{k \times k}$ which maintains the dimension.

Baseline RL algorithm. As baseline of deep RL algorithm, we use Proximal Policy Optimization (PPO) (Schulman et al., 2015) which is an on-policy actor-critic RL algorithm to learn policy $\pi_\theta(a | o)$ and value function V_θ with network parameter θ . Storing a set of recent transitions $\tau_t := (o_t, a_t, r_t, o_{t+1})$ in experience buffer \mathcal{D} , the network parameter θ is updated to maximize the following objective function:

$$L_{\text{PPO}}(\theta) = L_\pi(\theta) - \alpha L_V(\theta), \quad (1)$$

where α is a hyperparameter and some regularization terms are omitted. The clipped policy objective function L_π and value loss function L_V are defined as:

$$L_\pi(\theta) = \mathbb{E} \left[\min(\rho_t(\theta) \hat{A}_t, \text{clip}(\rho_t(\theta), 1 - \epsilon, 1 + \epsilon) \hat{A}_t) \right] \quad (2)$$

$$L_V(\theta) = \mathbb{E} \left[(V_\theta(o_t) - V_t^{\text{targ}})^2 \right], \quad (3)$$

where the expectation \mathbb{E} is taken with respect to $\tau \sim \mathcal{D}$, θ_{old} is the network parameter before the update, $\rho_t(\theta)$ is the importance ratio $\frac{\pi_\theta(a_t | o_t)}{\pi_{\theta_{\text{old}}}(a_t | o_t)}$, \hat{A}_t is advantage from Generalized Advantage Estimator (Schulman et al., 2015).

Overall framework. We propose two frameworks: InDA (Intra Distillation with Augmented observations) and ExDA (Extra Distillation with Augmented observations). To be specific, both of them use PPO for RL and the DA (Distillation with Augmented observation), described in Section 3.1, for regularization, although our frameworks can employ other RL algorithms and augmentation-based regularization. InDA, described in Section 3.2, interleaves PPO and DA, whereas ExDA, described in Section 3.3, performs PPO first then DA. As shown in Figure 1, we design InDA and ExDA to conduct either DA or PPO in each epoch.

3.1. Distillation with Augmented observations (DA)

DA regularizes reinforcement learning using distillation with data augmentation, where we train the network to output the same policies and values for given both original and augmented observations. To do so, we fix the network θ_{old} to be distilled, and store observation o_t sampled from $\pi_{\theta_{\text{old}}}$ and their augmentations $o'_t = \phi(o_t)$ in augmented buffer \mathcal{D}_ϕ , where $\phi : \mathbb{R}^{n \times n} \mapsto \mathbb{R}^{n \times n}$ is a transformation function. We then train a network θ to minimize the following distillation loss function:

$$L_{\text{DA}}(\theta) = L_{\text{PD}}(\theta) + L_{\text{VD}}(\theta), \quad (4)$$

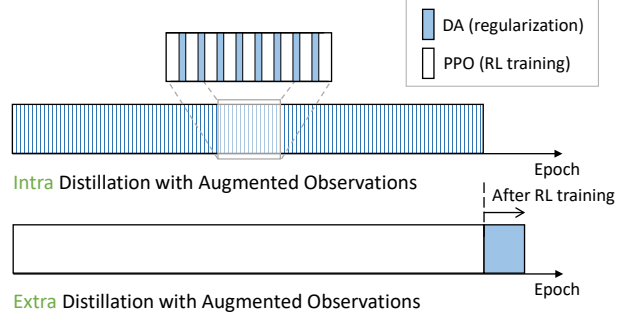


Figure 1. An illustration comparing InDA and ExDA

where L_{PD} is Kullback–Leibler divergence between policies $\pi_{\theta_{\text{old}}}$ and π_θ and L_{VD} is the mean-squared deviation between value functions $V_{\theta_{\text{old}}}$ and V_θ , i.e.,

$$L_{\text{PD}}(\theta) = \mathbb{E}_\phi [\text{KL}[\pi_{\theta_{\text{old}}}(\cdot | o_t), \pi_\theta(\cdot | o'_t)]] \quad (5)$$

$$L_{\text{VD}}(\theta) = \mathbb{E}_\phi [(V_{\theta_{\text{old}}}(o_t) - V_\theta(o'_t))^2] \quad (6)$$

The expectation \mathbb{E}_ϕ here is taken with respect to $\tau \sim \mathcal{D}_\phi$. Note that the augmented buffer \mathcal{D}_ϕ contains not only augmented observations but also original ones, and we freeze θ_{old} as trained in reinforcement learning. Hence, the distilled network θ behaves the same with θ_{old} for the original input images. This reduces the degeneration of training performance right after distillation. To our best knowledge, there is no prior work applying augmentation at this level of conservation of RL model. Another advantage of freezing θ_{old} is the reduced computational cost by pre-computing outcomes of θ_{old} in advance of DA, which is not available in other existing methods matching outputs of original and augmented inputs online (Raileanu et al., 2020).

3.2. Intra Distillation with Augmented observations

As described in Algorithm 1, InDA iteratively optimize PPO and DA, where we explicitly separate PPO and DA by phase. Such a separation reduces their interference (Hansen & Wang, 2020), while they are often optimized simultaneously in other methods (Raileanu et al., 2020). This phasic separation further robustifies our algorithm in addition to the conservative distillation of DA. We variate the timing of augmentation by S and T , which are the times of, respectively, starting and terminating DA. Also, we adjust the interval of distillation with I . Each DA phase, we compute $\pi_{\theta_{\text{old}}}$ and $V_{\theta_{\text{old}}}$ using $f_{\theta_{\text{old}}}$ which is trained until current DA phase. We provide further details on InDA in the supplementary material.

3.3. Extra Distillation with Augmented observations

As described in Algorithm 2, ExDA performs the distillation followed by the end of RL training, where the lengths of

Algorithm 1 InDA

```

1: Hyperparameter:  $S, T, N, I, \phi$ 
2: Initialize  $\theta$  close to origin.
3: for  $n = 1, 2, \dots, N$  do
4:   // RL training
5:   for  $i = 1, 2, \dots, I$  do
6:     Store sampled transitions to  $\mathcal{D}$ ;
7:     Optimize RL objective  $L_{\text{PPO}}(\theta)$  with  $\mathcal{D}$ ;
8:   end for
9:   // Distillation phase
10:  if  $n \in [S, T]$  then
11:    Store  $\theta_{\text{old}} \leftarrow \theta$ ;
12:    Generate  $\mathcal{D}_\phi$  by augmenting  $\mathcal{D}$  with  $\phi$ ;
13:    Minimize  $L_{\text{DA}}(\theta)$  with  $\mathcal{D}_\phi$ ;
14:  end if
15: end for

```

Algorithm 2 ExDA

```

1: Hyperparameter:  $N, M, \phi$ 
2: Initialize  $\theta$  close to origin.
3: //Pre-training phase with RL algorithm
4: for  $n = 1, 2, \dots, N$  do
5:   Store sampled transitions to  $\mathcal{D}$ ;
6:   Optimize RL objective  $L_{\text{PPO}}(\theta)$  with  $\mathcal{D}$ ;
7: end for
8: Store  $\theta_{\text{old}} \leftarrow \theta$ ;
9: // Distillation at the end of RL training
10: for  $m = 1, 2, \dots, M$  do
11:   Generate  $\mathcal{D}_\phi$  by augmenting  $\mathcal{D}$  with  $\phi$ ;
12:   Minimize  $L_{\text{DA}}(\theta)$  with  $\mathcal{D}_\phi$ ;
13: end for

```

DA and RL training are parameterized by M and N , respectively. It is worth to note that one can lower computational cost by replacing L_{DA} with L_{PD} in DA as there is no need of value function after DA. We empirically check that this reduction wouldn't degenerate RL performance. Besides, we consider the re-initialization after pre-training, because we expect that diminishing of non-stationarity can improve generalization as mentioned in (Igl et al., 2020). However, training performance is not preserved after re-initialization because $\pi_{\theta_{\text{old}}}$ is not completely distillation by low data diversity. Thus, we do not use re-initialization for DA. We leave more interesting details in the supplementary material.

4. Experiment

Setups. We evaluate the time-sensitivity of applying augmentation on OpenAI Procgen benchmark of 16 games, (Cobbe et al., 2020), where at each time t , visual observation o_t is given as an image of size 64×64 , and contains full or partial information on the system state. Training or

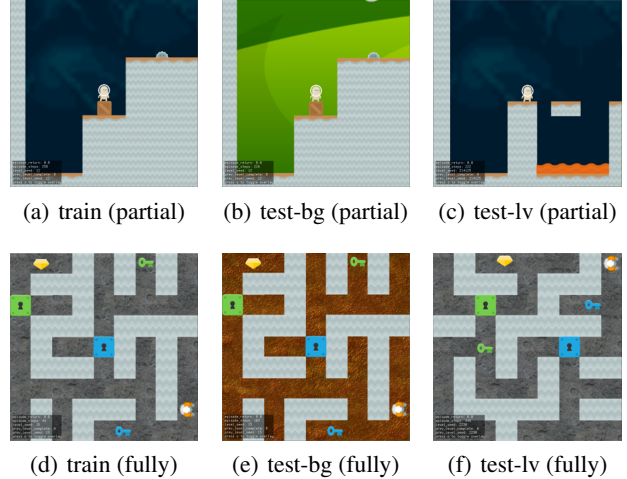


Figure 2. An example set of training and testing environments in Procgen benchmark: (upper row) an example of partially observable environment with Coinrun; (lower row) an example of fully observable environment with Heist; (left column) train: a set of levels and backgrounds for training; (center column) test-bg: the same training levels on unseen backgrounds; (right column) test-lv: a set of unseen levels on the same training backgrounds

testing environment is defined by a pair of game and mode, where mode determines a set of levels and backgrounds shown in the environment. As training environment, we use one of two modes: *easy* and *easybg*. Easy mode provided by Cobbe et al. (2020) contains a set of 200 levels, where an agent can learn basic dynamics of game and experience various backgrounds. To see clear advantage from visual augmentation, we further easicate easy mode and devise *easybg* mode of which only difference from easy mode is showing only a single background. To evaluate generalization capabilities, we use two modes: *test-bg* and *test-lv*, which contain unseen backgrounds and levels, respectively, in addition to the mode that we use for training. Fig 2 presents an example set of modes that we use in evaluation. The details of modes in our evaluation is provided in the supplementary material.

For the sake of clarity, we mainly focus on two visual augmentations each of which has clearly distinguishing inductive bias:

- (a) *Random convolution* transforms an image by passing a single convolutional layer initialized randomly (Lee et al., 2019). Augmentation with this can impose invariant behavior on color changes, and thus is anticipated to provide strong generalization on background changes.
- (b) *Crop* leaves a randomly selected rectangle and puts zero-pads to the outside (Raileanu et al., 2020). This

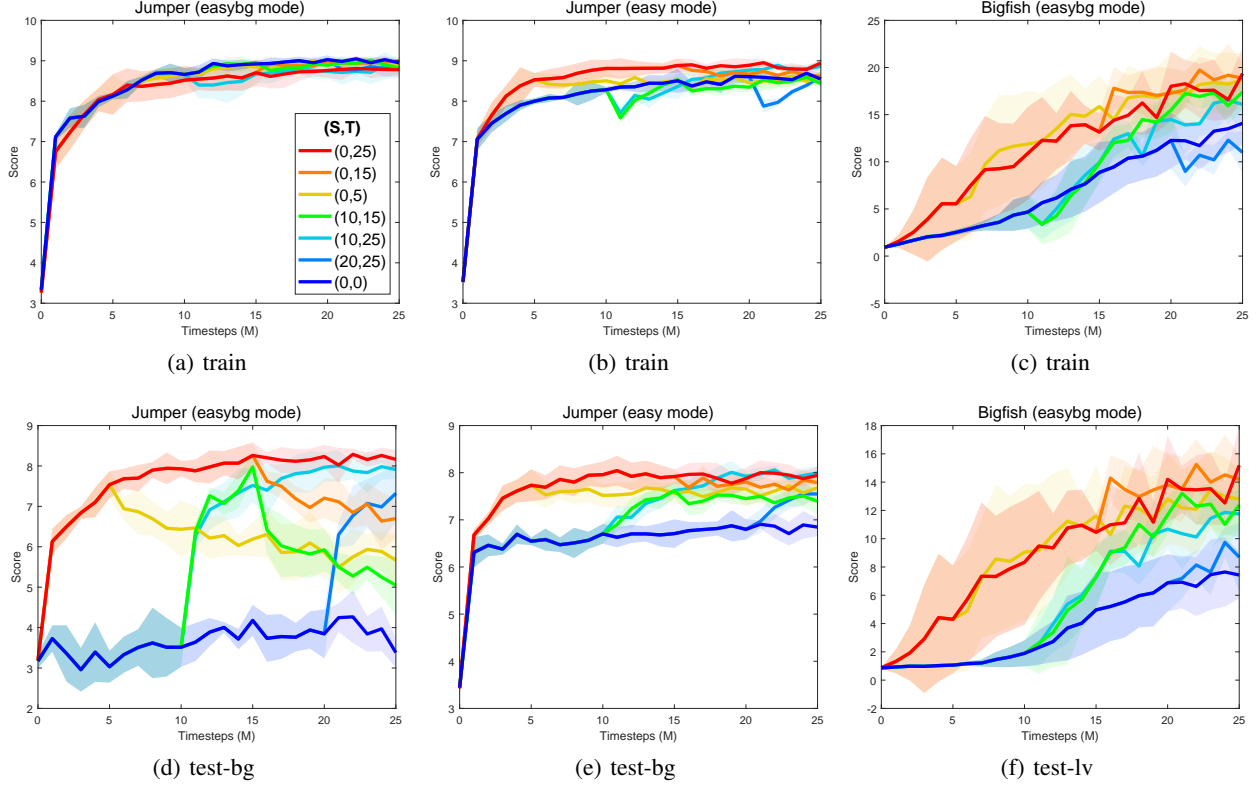


Figure 3. Comparison according to usage period of augmentation with InDA: (S, T) is hyper-parameters of InDA for a start and terminal time step of distillation. InDA uses random convolution on Jumper and crop on Bigfish as an augmentation method. Test results are evaluated on test-bg (unseen backgrounds) and test-lv (unseen levels). Shade region is a standard deviation of five runs. The difference between Jumper (easybg) and Jumper (easy) shows that the benefits of data efficiency and the maintenance of generalization can be differed by the diversity of factors in observations. For instance, when an agent is trained on Jumper (easybg mode), augmentation decreases the data efficiency at the curve $(0, 25)$ of (a). Moreover, they lose the generalization after the interruption at curves $(0, 5)$, $(0, 15)$ and $(10, 15)$ in (d). On the contrary, augmentation boosts the training $[(0, 25)$ of (b)] and maintains the generalization $[(0, 5)$, $(0, 15)$, $(10, 15)$ of (e)] despite augmentation interrupted on Jumper (easy mode). In addition, the delayed augmentation can improve data generalization as much as the curve $(0, 25)$ in the curves $(10, 25)$, $(20, 25)$. On the other hand, when the augmentation significantly accelerates the training, the early start of augmentation is essential for data efficiency and generalization because of limited data. Furthermore, the short-term augmentation can contribute to data efficiency and generalization such as the curves $(0, 5)$, $(10, 15)$ in Bigfish and Jumper (easy mode).

augmentation is particularly useful in the fully observable scenarios as it imposes an efficient attention mechanism.

We also report result with other visual augmentations including *color jitter*, *gray* and *cutout color* in the supplementary material, where the same main messages can be found. All results in the main paper are reported as averages over five runs.

4.1. Augmentation during RL training

Reinforcement learning has a non-stationarity, where the distribution of agent’s trajectory and policy are changing over time, but recently proposed data augmentation frameworks use augmented data in the whole training time. Furthermore,

augmentation does not always help train and test simultaneously, as the test environment has unseen challenges from training. Thus, we consider the necessity of using augmentation whole training time, even though RL has non-stationary characteristics. In this section, we want to find out when and how the agent is particularly helped by augmentation in RL training.

We variate the times to start and terminate distillation, denoted by S and T , respectively. We experiment by changing the distillation start time S and distillation terminal time T of InDA to see how generalization’s effect depends on the time to use augmentation. Compared to PPO, we evaluate InDA with six different pairs of start and terminal time of distillation (S, T) . When the training time steps are 25M, the six pairs (S, T) consist of $(0, 25)$, $(0, 5)$, $(0, 15)$, $(10, 0)$,

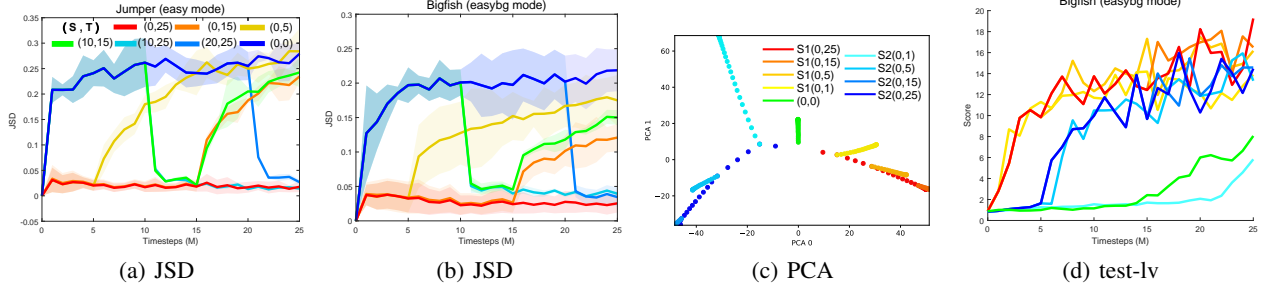


Figure 4. Comparison distance using Jensen-Shannon Divergence between policy from augmented observations and non-augmented observations in (a) Jumper(easy mode) with random convolution and (b) Bigfish (easybg mode) with crop. We compare different two Samples which trained on Bigfish (easybg mode) about test performance on unseen levels in (c) and optimizing trajectory in (d). Optimizing trajectory in (c) consists of scattered network parameters after dimension reduction using PCA.

(20, 0), (10, 15) and also PPO can be considered InDA with $(S, T) = (0, 0)$. We explained with Jumper and Bigfish in the main paper, and experiments on other environments are described in the supplementary material. Fig 3 represents three environments, Jumper with easy and easybg mode and Bigfish with easybg mode. In the following, we call the curve using a parameter (S, T) .

Interrupted augmentation. We wonder how generalization would change after regularization stopped. Thus, we stop the DA during training, such as (0, 5), (0, 15). When we compare the graph Fig 3(d) and Fig 3(e), generalization performance in Fig 3(d) rapidly decrease after interrupted on both (0, 5) and (0, 15). In contrast, the curves (0, 5) and (0, 15) in Fig 3(e) maintain the generalization in spite of interrupting augmentation. In training performance, InDA which uses augmentation throughout training, performs better than PPO in Fig 3(b); however, in Fig 3(a), augmentation does not improve the training performance. These results mean that the random convolution alleviates the difficulty by various backgrounds. On the contrary, random convolution can induce a growing difficulty by increasing the number of factors in a single background. Therefore, the generalization rapidly decreases after augmentation interrupted when training with a single background. On the other hand, the training can have help when their difficulty is solved by augmentation, such as Fig 3(b), Fig 3(c). Thus, in deep reinforcement learning, neural networks maintain the regularization when augmentation helps the training. Similarly, Golatkar et al. (2019) argued that the regularization biases toward regions of loss landscape have several equivalent generalized solutions. For the same reason, augmentation regularizes a neural network model by the bias toward generalization in deep reinforcement learning. Moreover, (0, 5), (0, 15) increase the training performance and generalization, similar to (0, 25), although they use augmented observations only for a while in Bigfish.

Delayed augmentation. We experiment on the general-

ization when we start to use augmentation lately as 10M, 20M. As shown in Fig 3(d) and Fig 3(e), the generalization rapidly increase after using augmentation at 10M and 20M. Although we use augmentation lately, augmentation helps the generalization regardless of the usage timing. (Golatkar et al., 2019) show that delayed augmentation cannot achieve as much as using augmentation during whole training in supervised-learning. However, (10, 25) improves generalization comparable with (0, 25), which use augmentation throughout training, unlike supervised learning. However, when augmentation largely helps the training, such as Fig 3(e), delayed augmentation struggle to follow earlier in Fig 3(f), because the reinforcement learning has the Markov property. Furthermore, unlike supervised learning, reinforcement learning has a limited number of samples, so using augmentation from the initial time is more critical than supervised learning if augmentation helps the training. We confirm that delayed augmentation can induce bias toward generalization after interrupted, although it is not used in initial transient time from (10, 15) at Fig 3(e), Fig 3(f). Through this result, augmentation inducing bias toward generalization can occur regardless of timing.

Generalization with augmented observations in RL. We mention that data augmentation causes the bias toward generalization. Thus, we examine how data augmentation improves the generalization during training. First, We compare the policy distances between augmented observations and non-augmented observations for each usage timing of augmentations in Fig 4(a) and Fig 4(b). We measure the policy distance using Jensen-Shannon Divergence because it is a lower bound for the joint empirical risk across non-augmented and augmented observations (Ilse et al., 2020; Raileanu et al., 2020). The policy distances are remarkably reduced when using augmentation in spite of delayed usage at (10, 25), (20, 25) in Fig 4(a) and Fig 4(b). Conversely,

the policy distances of (0, 5) and (0, 15) have a rapid increase after interrupted augmentation. Nevertheless, the generalization is similar with fully utilized augmentation such as (0, 25) in Fig 3(e) and Fig 3(f). This shows that the generalization about the change of backgrounds and levels is not relevant to policy consistency about augmented observations after generalization.

We analyze about two samples, which are trained on Big-fish environments, for verifying when generalization occurs. When using augmentation from the initial time, the rising time of performance differs for each sample in Fig 4(d). Sample 1 increases rapidly almost as soon as it starts, while Sample 2 begins to increase after learning about 5M. After 1M, 5M, and 10M, stopping augmentation increases the performance like non-interrupted, except when discontinued in 1M of Sample 2. Also, we draw the optimizing trajectories (Li et al., 2017) about each sample and PPO using PCA in Fig 4(c). The method of plotting trajectory is explained in the supplementary material in detail. Each sample learns through different learning paths from the randomly initialized point. We can see that the rest of the agents except Sample2’s (0, 1) and (0, 0) are biased toward the direction of generalization. Thus, augmentation causes bias toward generalization, but the learning path’s direction differs depending on the initial point. Furthermore, the time step to regularize by augmentation also differs in each seed.

As a result, the generalization is made by bias toward generalization while matching the policy between augmented observations and non-augmented observations. We need augmentation until biased toward generalization. However, the time to regularize is random according to the learning path. Thus, it is hard to decide when we can stop the augmentation.

Train	PPO	Oracle	InDA	ExDA
Coinrun	9.64 ± 0.07	7.11 ± 0.205	8.81 ± 0.992	9.44 ± 0.149
Fruitbot	29.78 ± 0.899	29.74 ± 0.443	26.17 ± 0.574	28.76 ± 0.789
Climber	12.34 ± 0.0833	9.78 ± 0.306	10.88 ± 0.162	12.07 ± 0.0726
Heist	8.99 ± 0.513	7.21 ± 0.27	5.15 ± 0.614	8.72 ± 0.533

Table 1. Comparison training performance: Training with random convolution in both ExDA and InDA. Oracle is trained using PPO on test environments. ExDA preserve the training performance of PPO rather than InDA, this shows that the augmentation can disturb the training. In addition, diverse backgrounds increase the difficulty of training as shown in Oracle.

Test	PPO	Oracle	InDA	ExDA
Coinrun	5.48 ± 0.583	7.11 ± 0.205	7.14 ± 0.479	7.8 ± 0.388
Fruitbot	10.83 ± 1.908	29.74 ± 0.443	21.93 ± 0.664	23.57 ± 0.745
Climber	1.97 ± 0.51	9.78 ± 0.306	7.36 ± 0.273	8.11 ± 0.457
Heist	5.18 ± 0.838	7.21 ± 0.269	4.96 ± 0.777	8.15 ± 0.633

Table 2. Comparison generalization on unseen backgrounds: Both ExDA and InDA improve the generalization, however, ExDA outperforms InDA because of gap of training performance.

4.2. Augmentation after RL training

Most methods using data augmentation in reinforcement learning use augmentation throughout the RL training. We showed that augmentation rapidly increases the generalization performance despite the late usage of augmentation in Fig 3. From these results, we consider that the possibility to improve generalization after training in reinforcement learning. To confirm the effect of augmentation after RL training, we compare ExDA with InDA, PPO (Schulman et al., 2017) and Oracle that trained on test environments. We train 200 levels of single background Procgen environments during 25M time-steps. In contrast, we train ExDA during 30 epochs with 0.5M time steps, after training with PPO for 20M time-steps. Further detail about implementation and hyper-parameter is described in the supplementary material.

Table 2 shows that ExDA outperforms InDA because after training can preserve the training performance while augmentation impedes the training when using it during training. ExDA also exceed the train and test performance of other baselines such as DrAC (Raileanu et al., 2020), Rand-FM (Lee et al., 2019), Rad (Laskin et al., 2020) on most environments which have help the generalization by random convolution. Especially in Table 1, Heist struggles to train the policy when augmentation is used during training. Moreover, ExDA is comparable with Oracle despite it trained with a single background. This result shows that various backgrounds are critical factors to hinder training. Thus, it is possible to choose training in a single background rather than in a different background in an environment where the difficulty rise due to various backgrounds is large. Furthermore, computation complexity is distinctly decreased when using ExDA rather than InDA, because InDA update for 25M augmented data while ExDA computes only 30 epochs with 0.5M. We describe the computation issue about both ExDA and InDA in the supplementary material.

However, using augmentation after training does not always

	PPO		InDA		ExDA	
Env	Train	Test	Train	Test	Train	Test
Maze	9.75	6.79	9.63	8.01	9.72	7.74
	± 0.0327	± 0.158	± 0.143	± 0.288	± 0.026	± 0.054
Heist	9.00	4.13	8.15	5.91	8.79	5.35
	± 0.513	± 0.146	± 0.570	± 0.516	± 0.424	± 0.220

Table 3. Comparison the performance: Training with crop in both ExDA and InDA and testing on unseen levels. InDA generalize better than ExDA, despite ExDA almost transfer the training performance of PPO.

provide a guarantee of improving generalization. In Table 3, ExDA improve generalization than PPO. However, InDA is better than ExDA despite low training performance in Table 3. The number of data is important for generalization of the level (Cobbe et al., 2020), and augmentation during training can increase observations’ diversity. Thus, augmentation after training is hard to get over the limitation of data diversity when the generalization needs the diversity of state distribution.

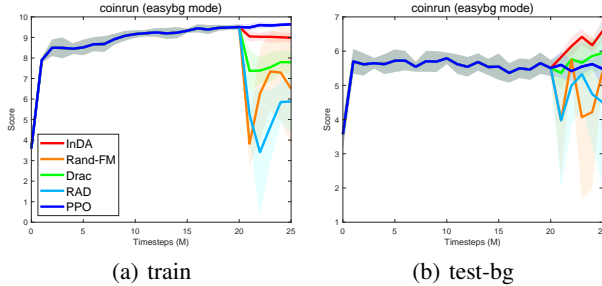


Figure 5. Comparison delayed augmentation with other baselines on Coinrun. The training performance degenerate after using augmentation in any methods, however, InDA is relatively stable rather than others.

Preserving the training performance after regularization. In ExDA, we transfer the policy after training 20M time steps with PPO. Thus, we explain why other augmentations are not used after pre-training. In Fig 5, we compare the results of training and test performance with Drac (Raileanu et al., 2020), Rand-FM (Lee et al., 2019), Rad (Laskin et al., 2020) when training 5M with each method after training 20M with PPO.

Every training curves decline immediately after starting the train at 20M in Fig 5(a). The objective function is changed to each baseline, and augmented data is newly added to data distribution. Thus, the optimizer should find a new optimal point for new objective function and data. During find the new optimal points, the agent learns in a different direction from the optimization direction in PPO. Thus, performance can be degraded because the learning direction on

loss landscape is different from maximizing rewards on non-augmented data in PPO. In spite of using self-supervised learning or representation learning, the policy is changed because they update the same network’s parameter for matching policy or latent features, such as s DrAC (Raileanu et al., 2020) and SODA (Hansen & Wang, 2020). However, InDA is more stable than the others because we distill the fixed policy and value in InDA. It does the stable training through conserving the policy on non-augmented observations during optimizing for augmented data. We confirm similar results on the other environments and compare them in the supplementary materials.

5. Discussion

We have studied the time-sensitivity of applying visual augmentation for RL, which is in contrast to that for SL, where such a difference can be explained with non-stationary data generation in RL. In particular, if the regularization imposed by augmentation is useful only for testing, it is better to procrastinate the augmentation to the end of RL training than to use it for the entire learning in terms of sample and computation complexity since it can disturb the RL training. However, an augmentation providing regularization useful in training obviously needs to be used during the whole training period to fully utilize its benefit in terms of not only generalization but also data efficiency. We believe that our findings provide useful insights not only for auto-augmentation adjusting the use of augmentation round-by-round, where DA at the end of RL training would provide substantial gains as ExDA does. However, it is still open to design auto-augmentation for RL as the gain from augmentation has highly non-stationary, and thus its evaluation is challenging.

References

- Achille, A., Rovere, M., and Soatto, S. Critical learning periods in deep networks. In *International Conference on Learning Representations*, 2018.
- Arora, S., Cohen, N., Hu, W., and Luo, Y. Implicit regularization in deep matrix factorization. In *Advances in Neural Information Processing Systems*, pp. 7411–7422, 2019.
- Auer, P. Using confidence bounds for exploitation-exploration trade-offs. *Journal of Machine Learning Research*, 3(Nov):397–422, 2002.
- Cobbe, K., Klimov, O., Hesse, C., Kim, T., and Schulman, J. Quantifying generalization in reinforcement learning, 2019.
- Cobbe, K., Hesse, C., Hilton, J., and Schulman, J. Leveraging procedural generation to benchmark reinforcement

- learning. In *International conference on machine learning*, pp. 2048–2056. PMLR, 2020.
- Erhan, D., Courville, A., Bengio, Y., and Vincent, P. Why does unsupervised pre-training help deep learning? In *Proceedings of the thirteenth international conference on artificial intelligence and statistics*, pp. 201–208. JMLR Workshop and Conference Proceedings, 2010.
- Espeholt, L., Soyer, H., Munos, R., Simonyan, K., Mnih, V., Ward, T., Doron, Y., Firoiu, V., Harley, T., Dunning, I., et al. Impala: Scalable distributed deep-rl with importance weighted actor-learner architectures. *arXiv preprint arXiv:1802.01561*, 2018.
- Farebrother, J., Machado, M. C., and Bowling, M. Generalization and regularization in dqn, 2020.
- Gidel, G., Bach, F., and Lacoste-Julien, S. Implicit regularization of discrete gradient dynamics in linear neural networks. In *Advances in Neural Information Processing Systems*, pp. 3196–3206, 2019.
- Golatkhar, A. S., Achille, A., and Soatto, S. Time matters in regularizing deep networks: Weight decay and data augmentation affect early learning dynamics, matter little near convergence. In *Advances in Neural Information Processing Systems*, pp. 10678–10688, 2019.
- Gunasekar, S., Woodworth, B. E., Bhojanapalli, S., Neyshabur, B., and Srebro, N. Implicit regularization in matrix factorization. In *Advances in Neural Information Processing Systems*, pp. 6151–6159, 2017.
- Hansen, N. and Wang, X. Generalization in reinforcement learning by soft data augmentation. *arXiv preprint arXiv:2011.13389*, 2020.
- Hansen, N., Sun, Y., Abbeel, P., Efros, A. A., Pinto, L., and Wang, X. Self-supervised policy adaptation during deployment. *arXiv preprint arXiv:2007.04309*, 2020.
- Higgins, I., Pal, A., Rusu, A. A., Matthey, L., Burgess, C. P., Pritzel, A., Botvinick, M., Blundell, C., and Lerchner, A. Darla: Improving zero-shot transfer in reinforcement learning, 2018.
- Igl, M., Farquhar, G., Luketina, J., Boehmer, W., and Whiteson, S. The impact of non-stationarity on generalisation in deep reinforcement learning. *arXiv preprint arXiv:2006.05826*, 2020.
- Ilse, M., Tomczak, J. M., and Forré, P. Designing data augmentation for simulating interventions. *arXiv preprint arXiv:2005.01856*, 2020.
- Kalashnikov, D., Irpan, A., Pastor, P., Ibarz, J., Herzog, A., Jang, E., Quillen, D., Holly, E., Kalakrishnan, M., Vanhoucke, V., et al. Qt-opt: Scalable deep reinforcement learning for vision-based robotic manipulation. *arXiv preprint arXiv:1806.10293*, 2018.
- Kostrikov, I., Yarats, D., and Fergus, R. Image augmentation is all you need: Regularizing deep reinforcement learning from pixels. *arXiv preprint arXiv:2004.13649*, 2020.
- Laskin, M., Lee, K., Stooke, A., Pinto, L., Abbeel, P., and Srinivas, A. Reinforcement learning with augmented data. *arXiv preprint arXiv:2004.14990*, 2020.
- Lee, K., Lee, K., Shin, J., and Lee, H. Network randomization: A simple technique for generalization in deep reinforcement learning. *arXiv*, pp. arXiv–1910, 2019.
- Li, H., Xu, Z., Taylor, G., Studer, C., and Goldstein, T. Visualizing the loss landscape of neural nets. *arXiv preprint arXiv:1712.09913*, 2017.
- Liu, Z., Li, X., Kang, B., and Darrell, T. Regularization matters in policy optimization – an empirical study on continuous control, 2020.
- Mnih, V., Kavukcuoglu, K., Silver, D., Rusu, A. A., Veness, J., Bellemare, M. G., Graves, A., Riedmiller, M., Fidjeland, A. K., Ostrovski, G., et al. Human-level control through deep reinforcement learning. *nature*, 518(7540): 529–533, 2015.
- Pinto, L., Andrychowicz, M., Welinder, P., Zaremba, W., and Abbeel, P. Asymmetric actor critic for image-based robot learning. *arXiv preprint arXiv:1710.06542*, 2017.
- Raileanu, R., Goldstein, M., Yarats, D., Kostrikov, I., and Fergus, R. Automatic data augmentation for generalization in deep reinforcement learning. *arXiv preprint arXiv:2006.12862*, 2020.
- Raparthi, S. C., Mehta, B., Golemo, F., and Paull, L. Generating automatic curricula via self-supervised active domain randomization, 2020.
- Schulman, J., Moritz, P., Levine, S., Jordan, M., and Abbeel, P. High-dimensional continuous control using generalized advantage estimation. *arXiv preprint arXiv:1506.02438*, 2015.
- Schulman, J., Wolski, F., Dhariwal, P., Radford, A., and Klimov, O. Proximal policy optimization algorithms. *arXiv preprint arXiv:1707.06347*, 2017.
- Silver, D., Schrittwieser, J., Simonyan, K., Antonoglou, I., Huang, A., Guez, A., Hubert, T., Baker, L., Lai, M., Bolton, A., et al. Mastering the game of go without human knowledge. *nature*, 550(7676):354–359, 2017.

- Silver, D., Hubert, T., Schrittwieser, J., Antonoglou, I., Lai, M., Guez, A., Lanctot, M., Sifre, L., Kumaran, D., Graepel, T., et al. A general reinforcement learning algorithm that masters chess, shogi, and go through self-play. *Science*, 362(6419):1140–1144, 2018.
- Srinivas, A., Laskin, M., and Abbeel, P. Curl: Contrastive unsupervised representations for reinforcement learning, 2020.
- Stooke, A., Lee, K., Abbeel, P., and Laskin, M. Decoupling representation learning from reinforcement learning. *arXiv preprint arXiv:2009.08319*, 2020.
- Tobin, J., Fong, R., Ray, A., Schneider, J., Zaremba, W., and Abbeel, P. Domain randomization for transferring deep neural networks from simulation to the real world. In *2017 IEEE/RSJ International Conference on Intelligent Robots and Systems (IROS)*, pp. 23–30. IEEE, 2017.
- Wu, X., Dyer, E., and Neyshabur, B. When do curricula work?, 2020.
- Yarats, D., Zhang, A., Kostrikov, I., Amos, B., Pineau, J., and Fergus, R. Improving sample efficiency in model-free reinforcement learning from images, 2020.
- You, K., Long, M., Wang, J., and Jordan, M. I. How does learning rate decay help modern neural networks?, 2019.

A. Modified Procgen Environments

This section explains Modified Procgen Environments, which is designed to verify different types of generalization, backgrounds, and levels. Open AI Procgen environments (Cobbe et al., 2020) share background themes such as *space_backgrounds*, *platform_backgrounds*, *topdown_backgrounds*, *water_backgrounds*, *water_surface_backgrounds*. We create new difficulties as *Easybg*, *Easybg-test*, *Easy-test*. *Easybg* generates environments which contain only one for each background, wall and agent theme. *Easybg-test* and *Easy-test* are for test about background change after trained on *Easybg* and *Easy*. Wall theme in (Climber, Coinrun, Jumper, Ninja) and Agent theme in (Climber, Coinrun) also compose with only one image resource in *Easybg*. Furthermore, We fix the exit_wall.choice and enemy theme in Dodgeball. We describe the usage themes in each environments, which are grouped by backgrounds theme as below:

- *space_backgrounds* (Bossfight, Starpilot)
Background: "space_backgrounds/deep_space_01.png"
- *platform_backgrounds* (Caveflyer, Climber, Coinrun, Jumper, Miner, Ninja)
Background: "platform_backgrounds/alien_bg.png", Coinrun (Agent color: Beige, Wall themes: Dirt), Climber (Agent color: Blue, Wall themes: tileBlue), Jumper (Wall theme: tileBlue), Ninja (Wall theme: bricksGrey)
- *topdown_backgrounds* (Chaser, Dodgeball, Fruitbot, Heist, Leaper, Maze)
Background: "topdown_backgrounds/floortiles.png", Dodgeball (Enemy theme: "misc_assets/character1.png", Exit_wall.choice: 0)
- *water_backgrounds* (Bigfish)
Background: "water_backgrounds/water1.png"
- *water_surface_backgrounds* (Plunder)
Background: "water_backgrounds/water1.png"

Easybg-test uses backgrounds in each background group, except the one used in *Easybg*. *Easy-test* is only defined for Climber, Jumper, Ninja, and they compose with *topdown_backgrounds*.

B. Implementation details

In this section, we explain about InDA, ExDA and other baselines. We train the agent with IMPALA-CNN (Espeholt et al., 2018) in every experiment.

B.1. InDA

We use PPO (Schulman et al., 2017) as base RL algorithms, For data efficiency, we store the observations during RL training in buffer \mathcal{D}_O . Before DA phase, we also make policy buffer \mathcal{D}_Π , value function buffer \mathcal{D}_V and augmented observation buffer \mathcal{D}_ϕ for distillation, because we only use one network model. We randomly sample pairs of (o, π, V) from buffer, and minimize loss function $L_{DA}(\theta)$. We reuse the sample three times like PPO, it can be controlled by # Epochs of DA. We did a greed searches for learning rate of DA $l_{DA} \in [1 \times 10^{-3}, 5 \times 10^{-4}, 2 \times 10^{-4}, 1 \times 10^{-4}, 5 \times 10^{-5}]$ and interval $I \in [1, 5, 10]$ and found the best combination $l_{DA} = 10^{-4}$ and interval $I = 5$. We fix the buffer size $\mathcal{D}_O = 40960$, because we collect the observations during five RL phases ($5 \times 256 \times 32$). We describe the every hyperparameter in Table 4.

B.2. ExDA

In ExDA, we generate and store (o, π, V) using $f_{\theta_{old}}$ in buffer \mathcal{D} . The optimal buffer size depends on the episode length of each environment. However, we standardize the buffer size as 0.5M in every environment. We augment the observation with three epochs intervals when using randomized augmentation methods. We did greed searches for # minibatches $[1024, 2048, 4096]$ and learning rate $[5 \times 10^{-4}, 1 \times 10^{-3}, 2 \times 10^{-3}]$. As a result, we select # of minibatches 4096 and a learning rate $1e - 3$. We describe every hyperparameter in Table 5:

Hyperparameter	Value
γ	0.999
λ	0.95
# Timesteps per rollout	256
# Epochs per rollout	3
# Minibatches per epoch	8
Reward Normalization	Yes
# Workers	1
# Environments per worker	32
Total timesteps	25M
LSTM	No
Frame Stack	No
Optimizer	Adam optimizer
Entropy bonus	0.01
PPO clip range	0.2
Learning rate	5×10^{-4}
Interval I	5
Size of \mathcal{D}_O	40960
# Epochs of DA	3
Learning rate of DA l_{DA}	1×10^{-4}
Image transformation ϕ	Any augmentation

Table 4. Hyperparameter for InDA

Hyperparameter	Value
Size of \mathcal{D}_O	0.5M
# Epoch	30
# Minibatches per epoch	4096
Learning rate	1×10^{-3}
# Workers	1
Optimizer	Adam optimizer
Image transformation ϕ	Any augmentation

Table 5. Hyperparameter for ExDA

B.3. Baselines

We compare ExDA and InDA with PPO (Cobbe et al., 2020), DrAC (Raileanu et al., 2020), Rand-FM (Lee et al., 2019), RAD (Laskin et al., 2020). Every baseline are based on PPO (Cobbe et al., 2020) and we adopt the implementation of PPO in (Cobbe et al., 2020).

- DrAC (Raileanu et al., 2020) regularizes both policy and value function as self-supervised learning. Regularization term have hyperparameter α_r for ratio with PPO objective. We use the hyperparameter recommended by the author.
- Rand-FM (Lee et al., 2019) is composed with random convolution networks and feature matching. They also need hyperparameter β for ratio between feature matching and PPO objective. We use same β with author.
- RAD (Laskin et al., 2020) naively use augmented observations in state distribution. Thus, there are no additional hyperparameters.

We describe the hyperparameter of baselines in Table 6.

Hyperparamter	Value
γ	0.999
λ	0.95
# of timesteps per rollout	256
# of epochs per rollout	3
# of Minibatches per epoch	8
Reward Normalization	Yes
# of Workers	1
# of environments per worker	64
Total timesteps	25M
LSTM	No
Frame Stack	No
Optimizer	Adam optimizer
Entropy bonus	0.01
PPO clip range	0.2
Learning rate	5×10^{-4}
α_r (DrAC)	0.1
β (Rand-FM)	0.002

Table 6. Hyperparameter for baseline algorithms

C. Data augmentation

In our experiments, we use five augmentation methods: *crop*, *grayscale*, *cutout color*, *random convolution* and *color jitter*. We refer the implementation of augmentations from Lee et al. (2019) (*random convolution*), Laskin et al. (2020) (*cutout color*, *color jitter*) and Raileanu et al. (2020) (*grayscale*, *crop*). We expect the generalization about background change from *random convolution*, *color jitter*, *gray*, *cutout color*. About the change of levels, we use *crop* and *cutout color* for generalization. Examples of data augmentation are represented below:

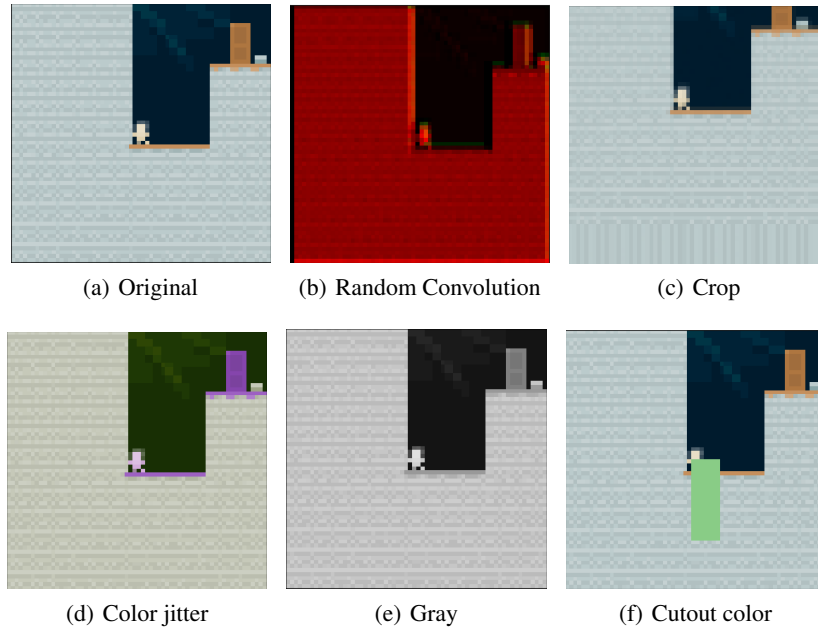


Figure 6. Examples of visual augmentations

D. Robustness in loss function change

In this sections, we show the training and test performance of delayed augmentations with other baselines such as DrAC (Raileanu et al., 2020), Rand-FM (Lee et al., 2019), RAD (Laskin et al., 2020). We use random convolution and crop as data augmentation methods, and we do not compare with RAD when we use crop in Fig 9 and Fig 10. The *crop* method used in our paper do not work well in RAD, because they use a different crop method with (Raileanu et al., 2020) in their paper (Laskin et al., 2020). As mentioned in Fig 5, InDA is more stable than others in training, and it affects generalization performance.

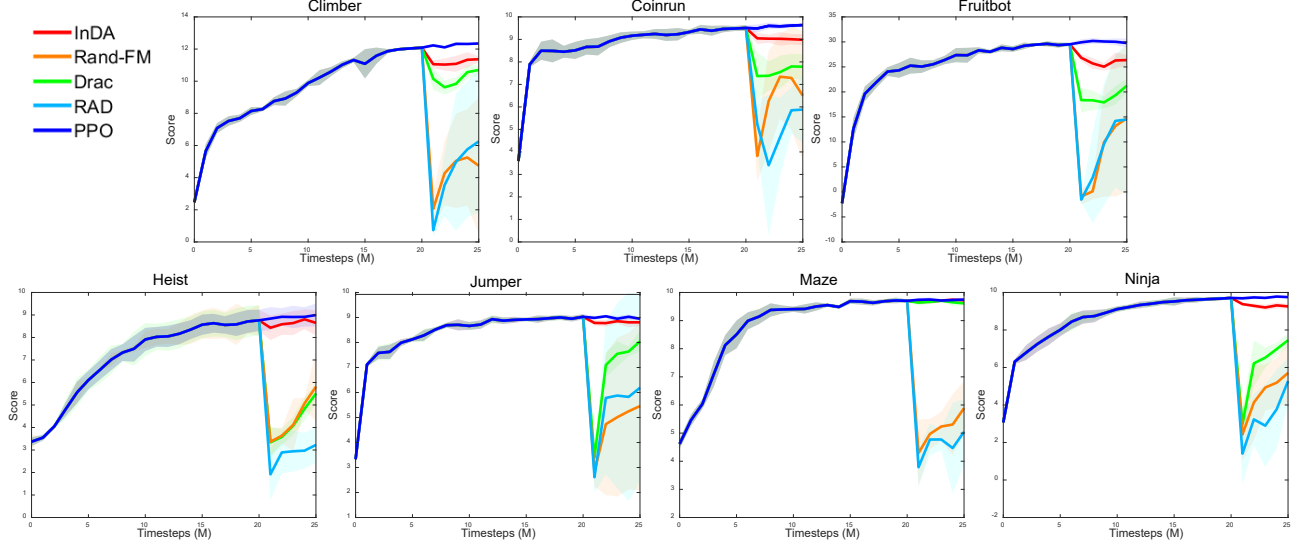


Figure 7. Comparison training performance of delayed augmentation with other baselines when using *random convolution* as an augmentation method.

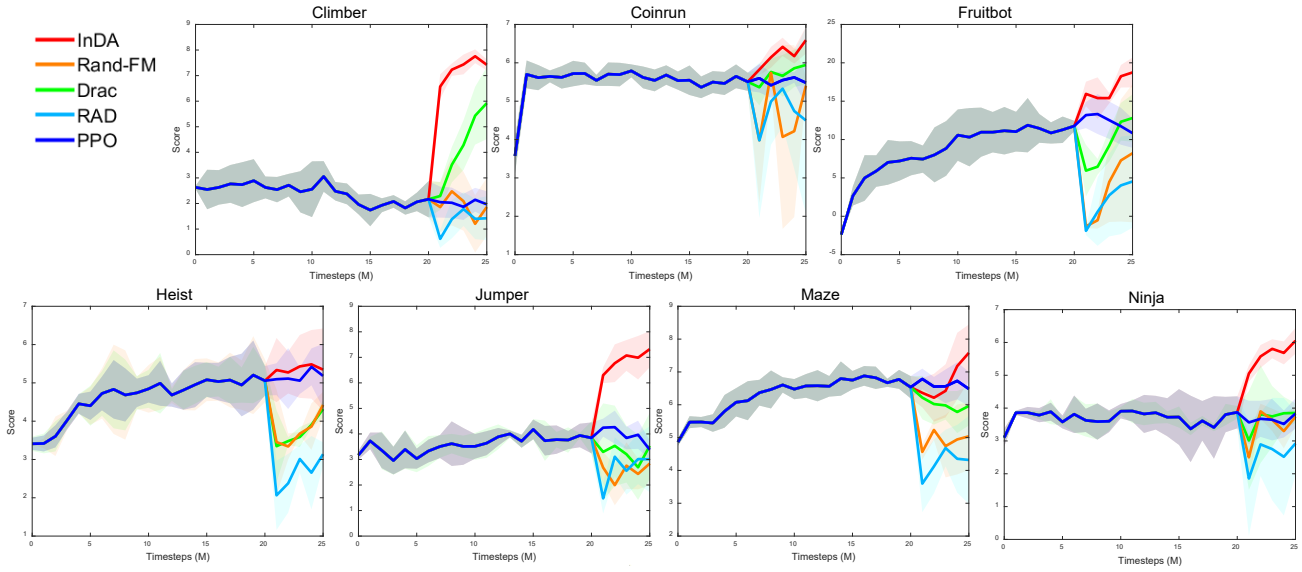


Figure 8. Comparison test performance of delayed augmentation with other baselines when using *random convolution* as an augmentation method.

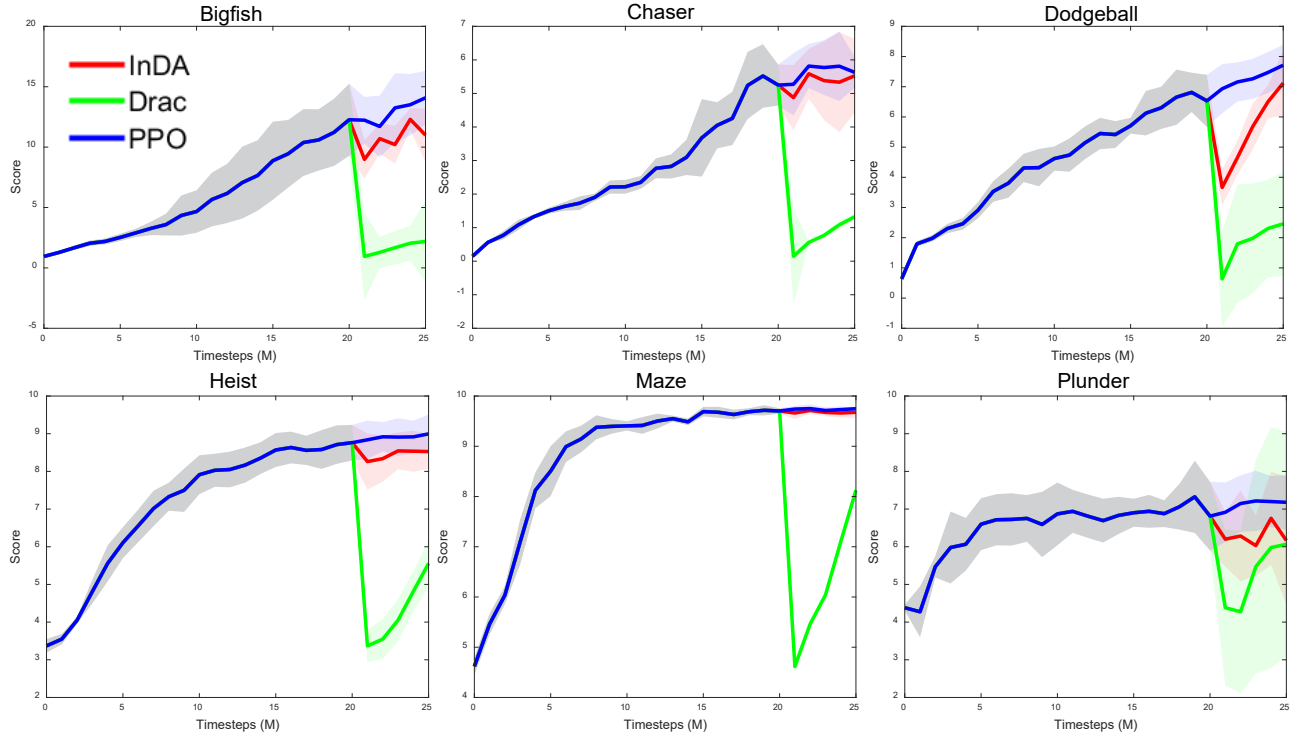


Figure 9. Comparison training performance of delayed augmentation with DrAC when using *crop* as an augmentation method.

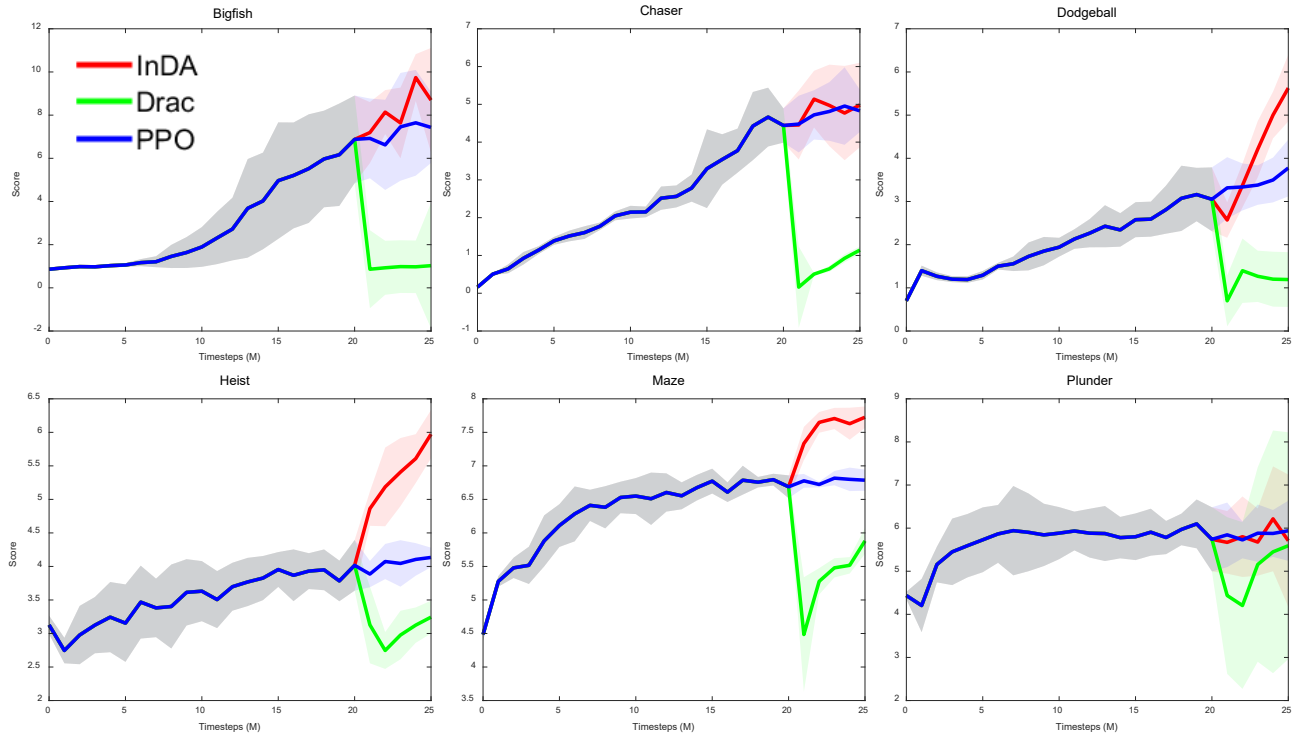


Figure 10. Comparison test performance of delayed augmentation with DrAC when using *crop* as an augmentation method.

E. Ablation study of ExDA

E.1. Initialization and regularization term

In this section, we do an ablation study about the factor of ExDA. We mention the loss function and re-initialization issue in Sec 3.3. The ExDA does not have to minimize L_{VD} because the value function is useless after RL training. The below results show that the L_{VD} cannot give any benefit in ExDA. Thus we only use L_{PD} for computational complexity. Furthermore, we also compare to verify the effect of non-stationarity with a re-initialized agent before distillation. Igl et al. (2020) argued that the non-stationarity causes the reduction of generalization. However, the re-initialization is not critical in test performance, as shown in Fig 12. Moreover, sometimes re-initialization makes it difficult to distill training performance such as Fruitbot and Ninja in Fig 11. We use *random convolution* as an augmentation method in here.

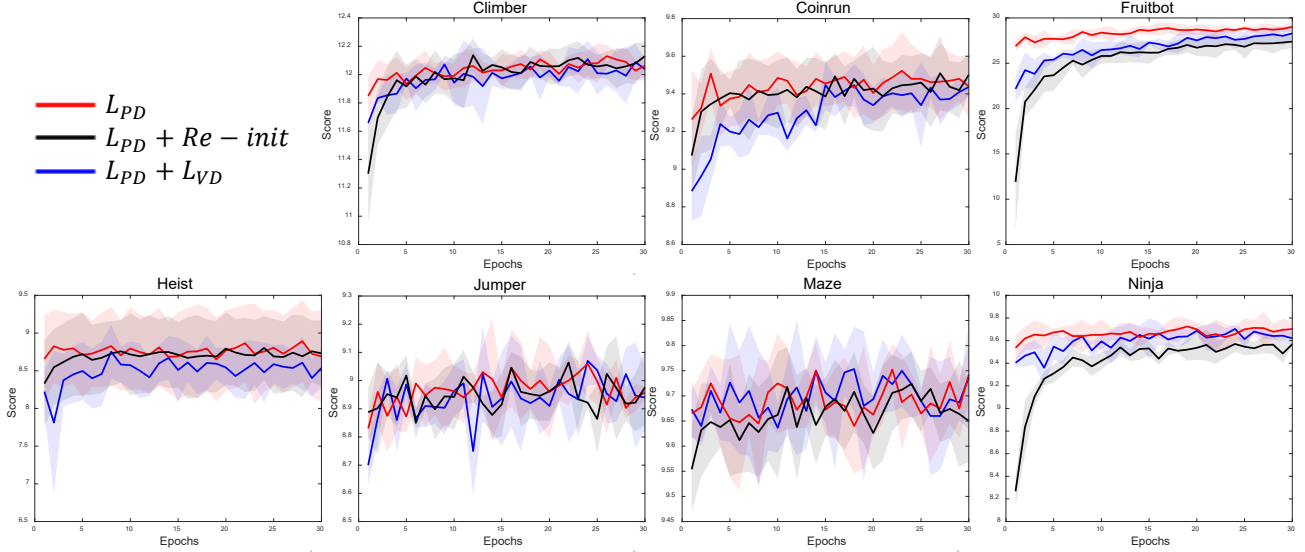


Figure 11. Training performance of ExDA with re-initialization or regularization with value function.

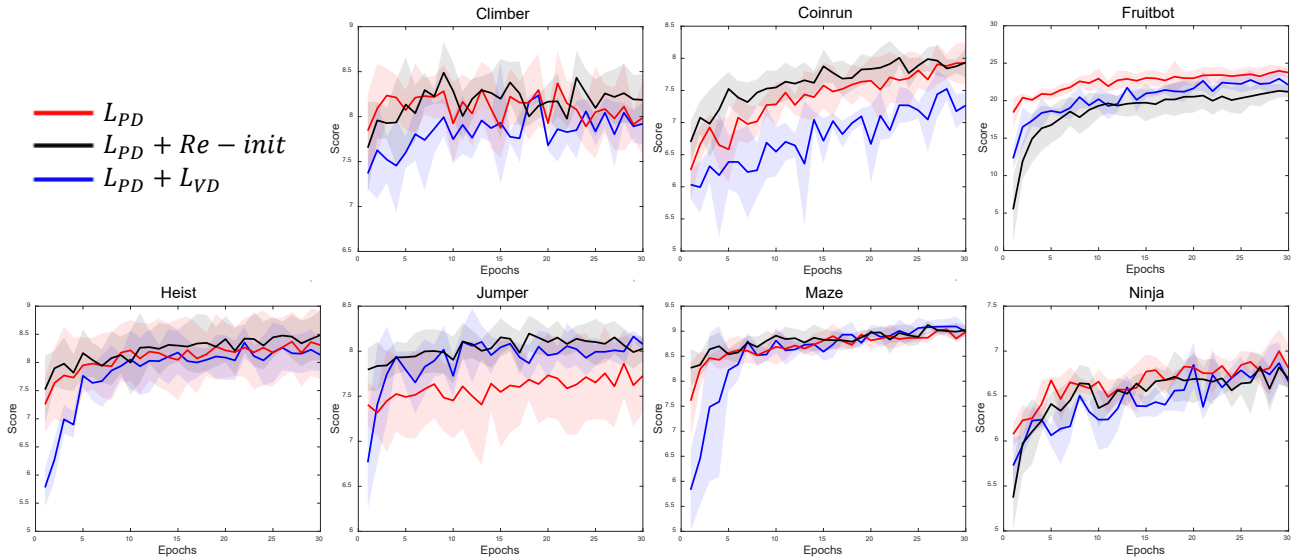


Figure 12. Test performance of ExDA with re-initialization or regularization with value function on unseen backgrounds.

E.2. ExDA after InDA with various backgrounds

When augmentation helps the training, ExDA struggle to follow the training performance of InDA because ExDA’s training performance is limited by pre-trained agent’s policy. Thus, we use InDA for ExDA’s pre-training, and call it as ExDA (InDA). As shown in Table 8, ExDA (InDA) is comparable to InDA, but not beyond. Thus, unless there is a meaningful difference in training performance, ExDA has no better generalization than InDA. However, in computational complexity, ExDA is more efficient than others such as InDA and DrAC when they have a similar performance. In the following section, we discuss about computational complexity.

Easy	PPO	InDA	ExDA (PPO)	ExDA (PPO) + reinit	ExDA (InDA)	ExDA (InDA) + reinit
Jumper	8.55	8.94	8.5	8.6	8.83	8.83
	± 0.17	± 0.09	± 0.183	± 0.156	± 0.215	± 0.126
Ninja	7.49	8.88	7.03	7.23	8.71	8.56
	± 0.42	± 0.34	± 0.058	± 0.159	± 0.344	± 0.394
Climber	8.63	8.5	8.1	8.09	8.16	7.99
	± 0.46	± 0.29	± 0.268	± 0.268	± 0.441	± 0.383

Table 7. The comparison with diverse agents which are trained with ExDA

Easy	PPO	InDA	ExDA (PPO)	ExDA (PPO) + reinit	ExDA (InDA)	ExDA (InDA) + reinit
Jumper	6.85	7.94	7.54	7.48	7.98	7.67
	± 0.19	± 0.19	± 0.158	± 0.154	± 0.148	± 0.155
Ninja	6.29	6.5	5.56	5.73	6.27	5.94
	± 0.19	± 0.19	± 0.158	± 0.154	± 0.148	± 0.155
Climber	6.96	7.28	7.06	6.89	6.8	5.45
	± 0.65	± 0.35	± 0.541	± 0.237	± 0.441	± 0.383

Table 8. Test performance of agents, which is trained on easy mode with random convolution.

E.3. Computational complexity

We compare the computational complexity with ExDA and InDA. InDA do DA for every 25M observations during training and reuse the sample in three times. However, ExDA only use 0.5M for DA during 30 epochs. Thus, ExDA is almost 5 times more efficient than InDA by roughly calculation. Furthermore, the ExDA save the time for augmentation comparing to InDA. When we train with same computational setting (GPU: GeForce RTX 2080 TI), ExDA only consumes 5 hours + 2 hours (PPO) when using random convolution, but, InDA consumes 18 hours. Thus, we recommend ExDA when InDA cannot give meaningful gain in training performance.

F. Time matter in training

This section shows every result of Fig 3 about time dependency with InDA. We experiment with *random convolution*, *crop*, *color jitter*, *gray*, *cutout color* and evaluate the test on unseen backgrounds (*random convolution*, *color jitter*, *gray*, *cutout color*) and levels (*random crop*, *cutout color*). However, the effect of generalization is hard to recognize in most cases, as shown in Appendix G. Thus, we mainly discuss the most effective augmentation, such as random convolution and crop in the main paper, and only represent some environments that have helped the generalization by color jitter, gray, and cutout color. *easybg* mode is used as default mode with three *easy* mode (Climber, Jumper, Ninja) in our experiments. The shaded regions and solid line represent the standard deviation and mean, across five runs (*random convolution*, *crop*) and three runs (*color jitter*, *cutout color*, *gray*).

F.1. Random convolution

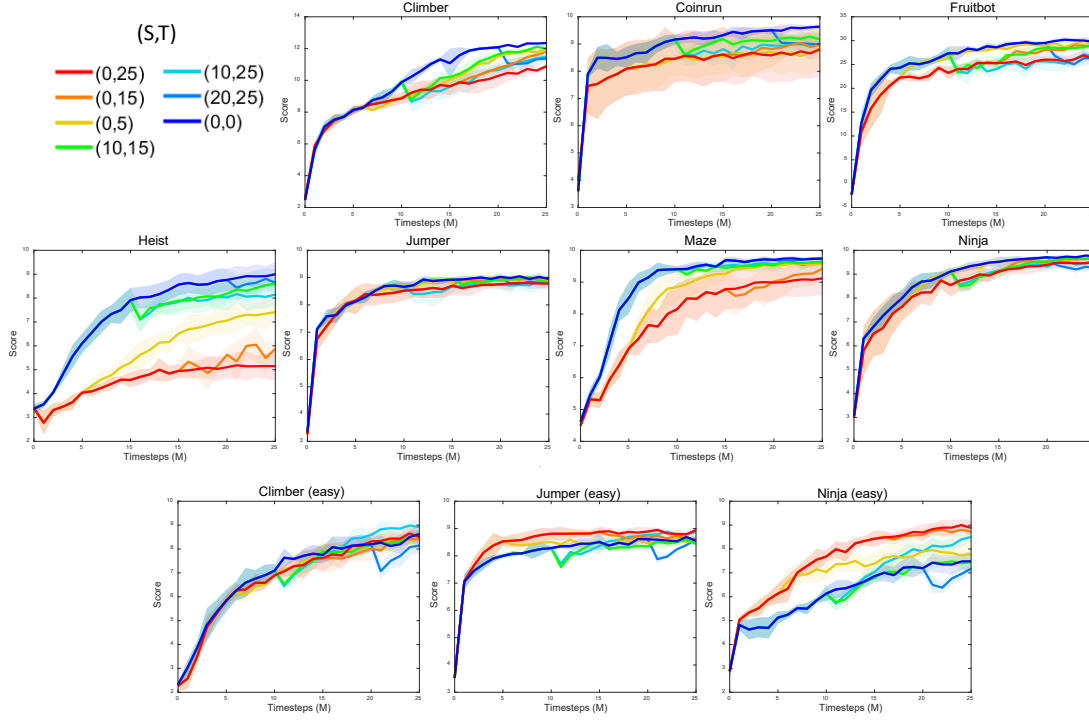


Figure 13. Comparison training performance according to usage period of augmentation with InDA (*random convolution*): The *easybg* is disturbed by *random convolution*, but, *easy mode* is improved training performance by *random convolution*.

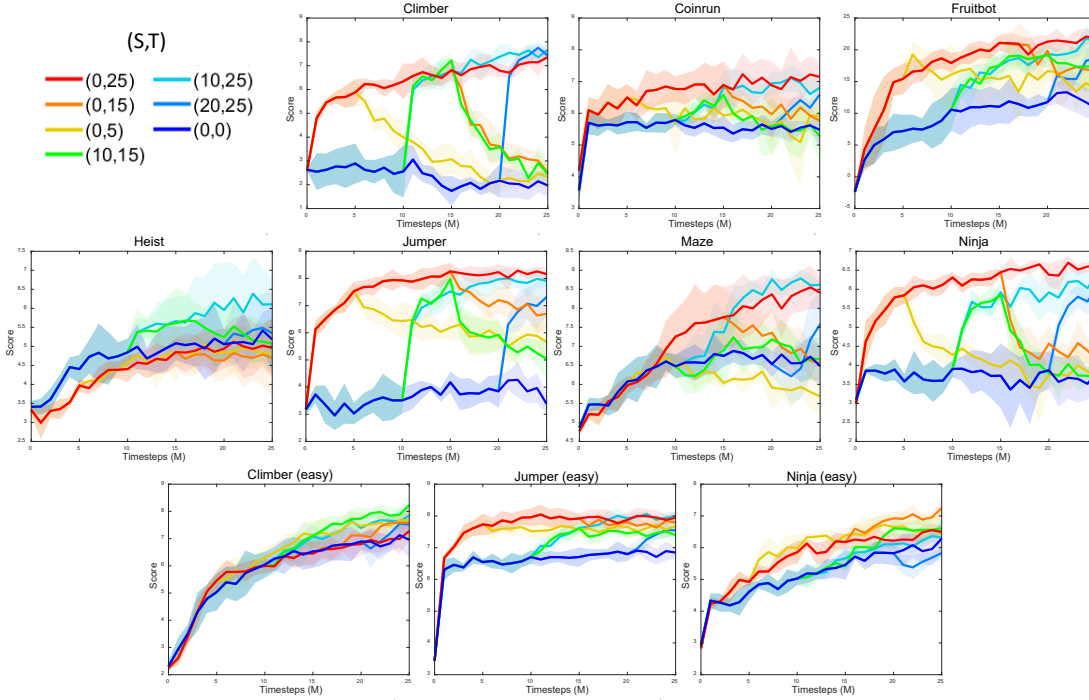


Figure 14. Comparison generalization on unseen backgrounds according to usage period of augmentation with InDA (*random convolution*): Most cases' tendencies are coincidence with the jumper, which is mentioned in the main paper..

F.2. Crop

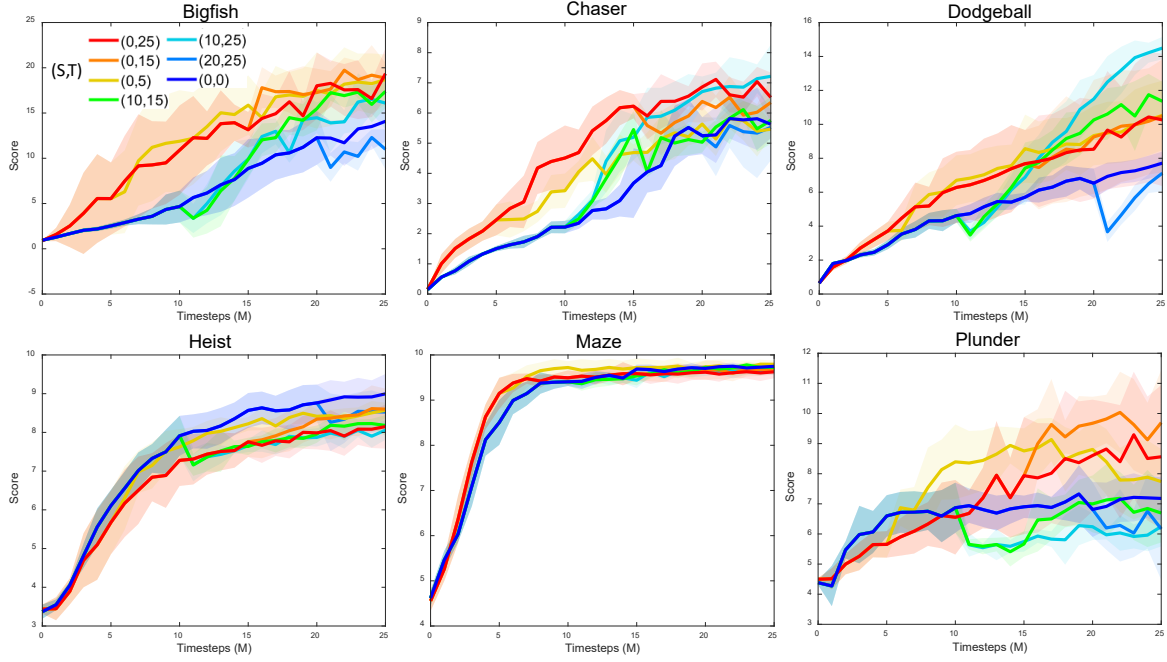


Figure 15. Comparison training performance according to usage period of augmentation with InDA (*crop*): *Crop* improve the training performance in Bigfish, Chaser, Dodgeball, Plunder. Furthermore, interrupted augmentation is also improved similarly with (0, 25).

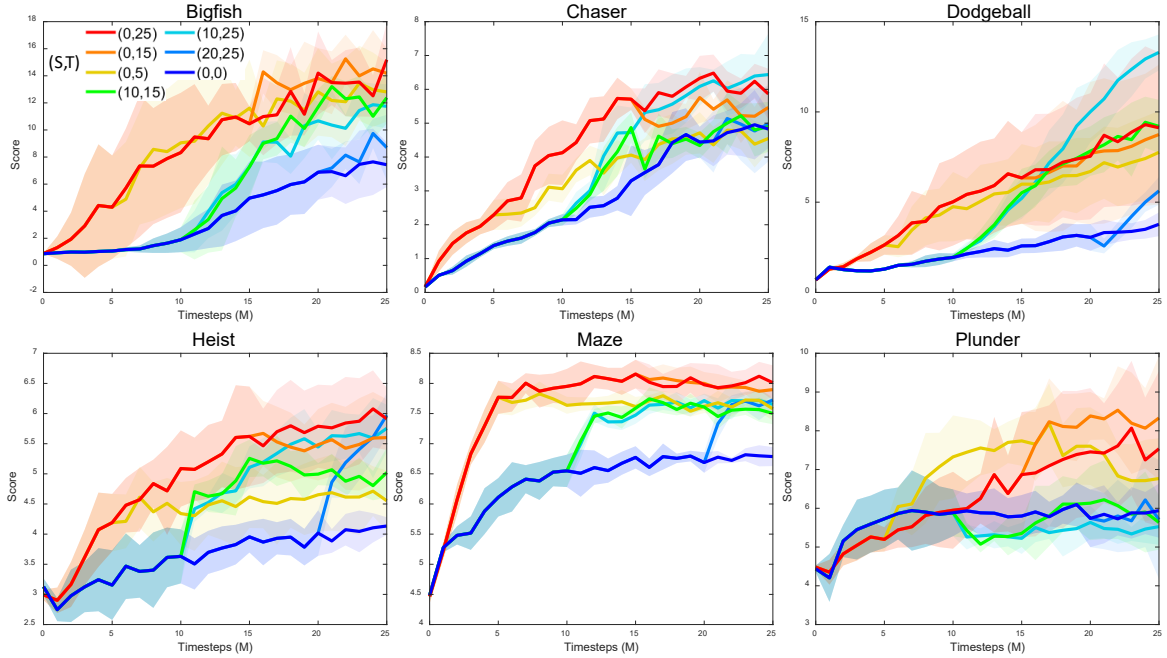


Figure 16. Comparison generalization on unseen levels according to usage period of augmentation with InDA (*crop*): The generalization is improved by *crop*, and it is conserved after interrupted in Heist and Maze. Bigfish, Chaser, Dodgeball, and Plunder have similar curves with training.

E.3. Color jitter

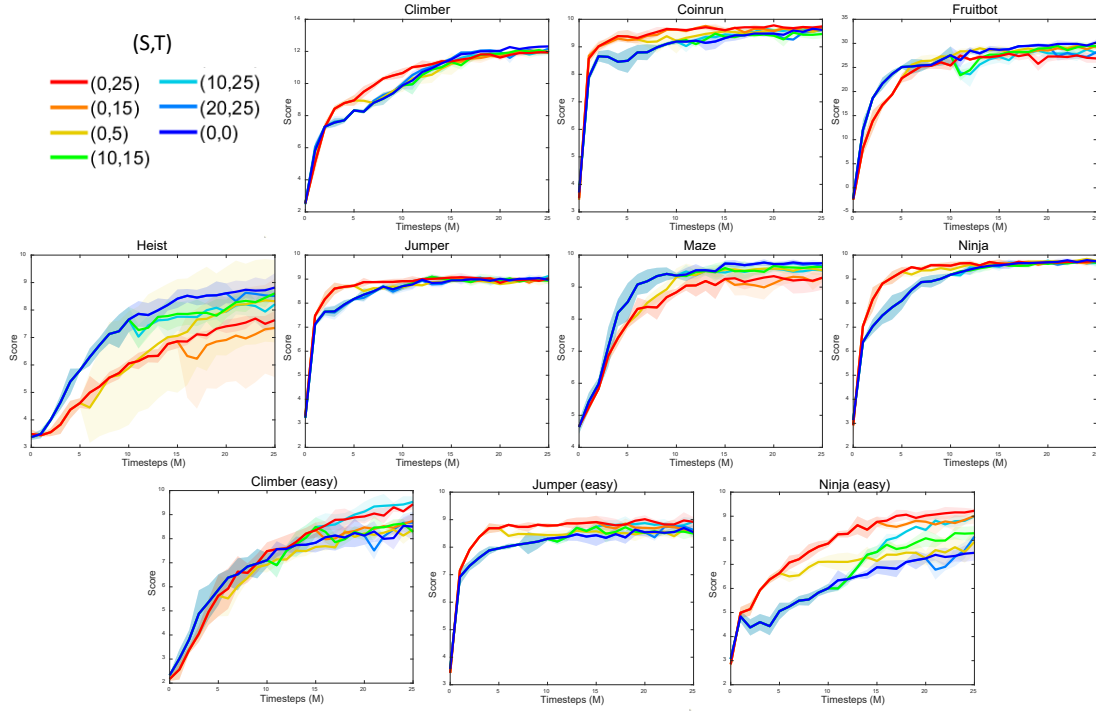


Figure 17. Comparison training performance according to usage period of augmentation with InDA (*color jitter*): *Color jitter* does not impede the training as much as *random convolution* in most environments. However, *color jitter* helps the training in easy mode.

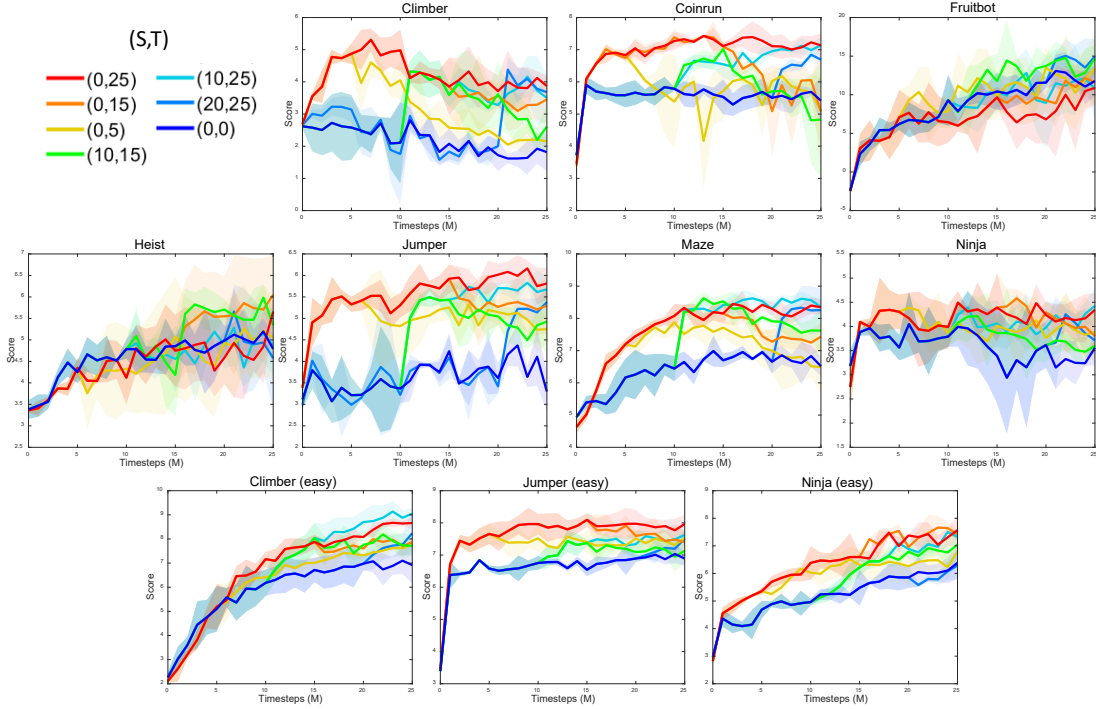


Figure 18. Comparison generalization on unseen backgrounds according to usage period of augmentation with InDA (*color jitter*): Test performance is influenced by *color jitter* as the trend, which is similar to *random convolution*.

F.4. Gray

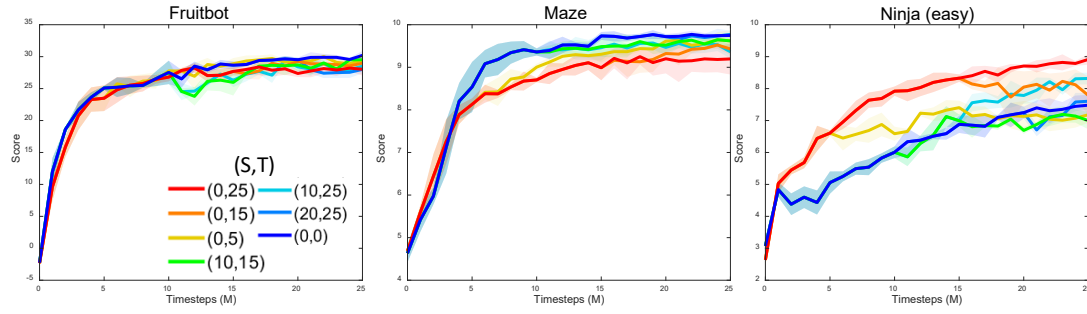


Figure 19. Comparison training performance according to usage period of augmentation with InDA (*gray*): The effect of *gray* is similar to *color jitter*.

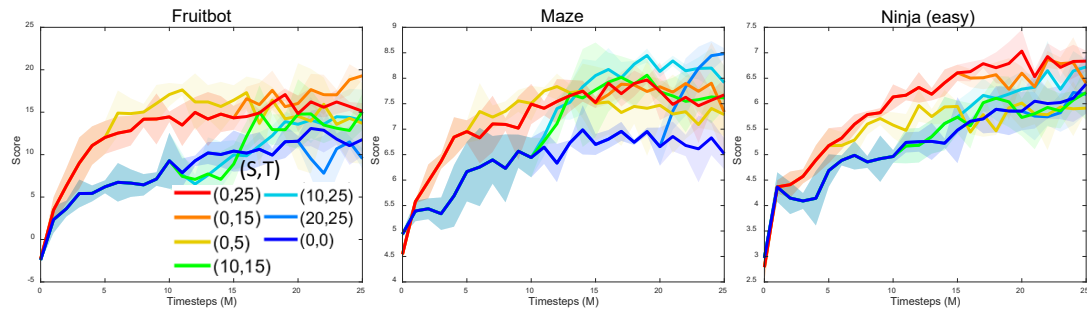


Figure 20. Comparison generalization on unseen backgrounds according to usage period of augmentation with InDA (*gray*): *Gray* improves the generalization, even if the usage of augmentation is delayed. However, it is hard to recognize by low effectiveness of *gray*.

F.5. Cutout color

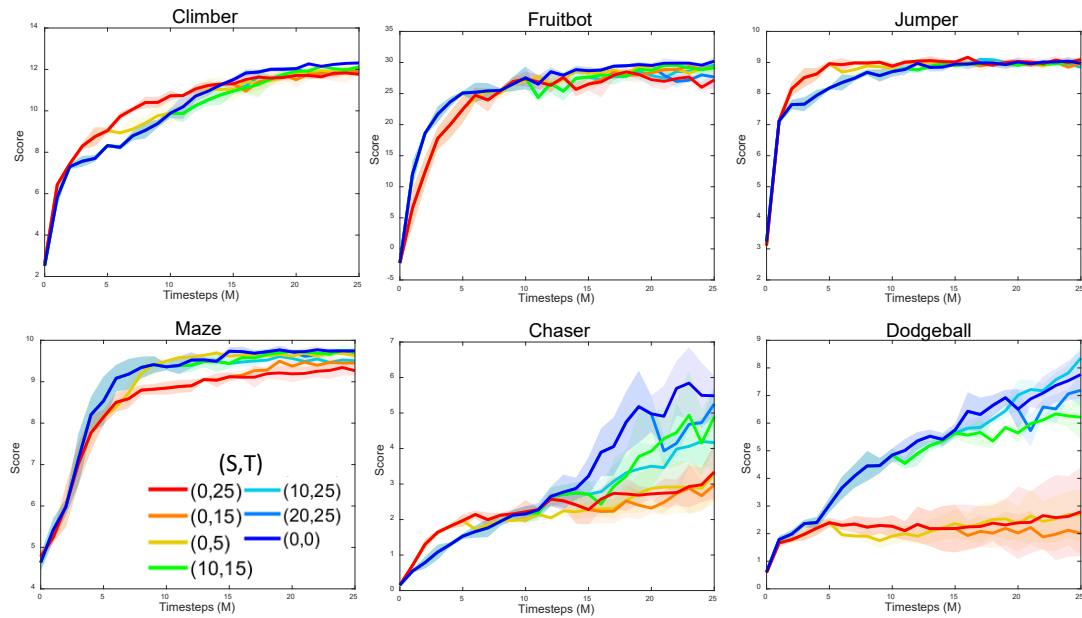


Figure 21. Comparison training performance according to usage period of augmentation with InDA (*cutout color*): *Cutout color* impedes the training, especially Chaser and Dodgeball are ruined.

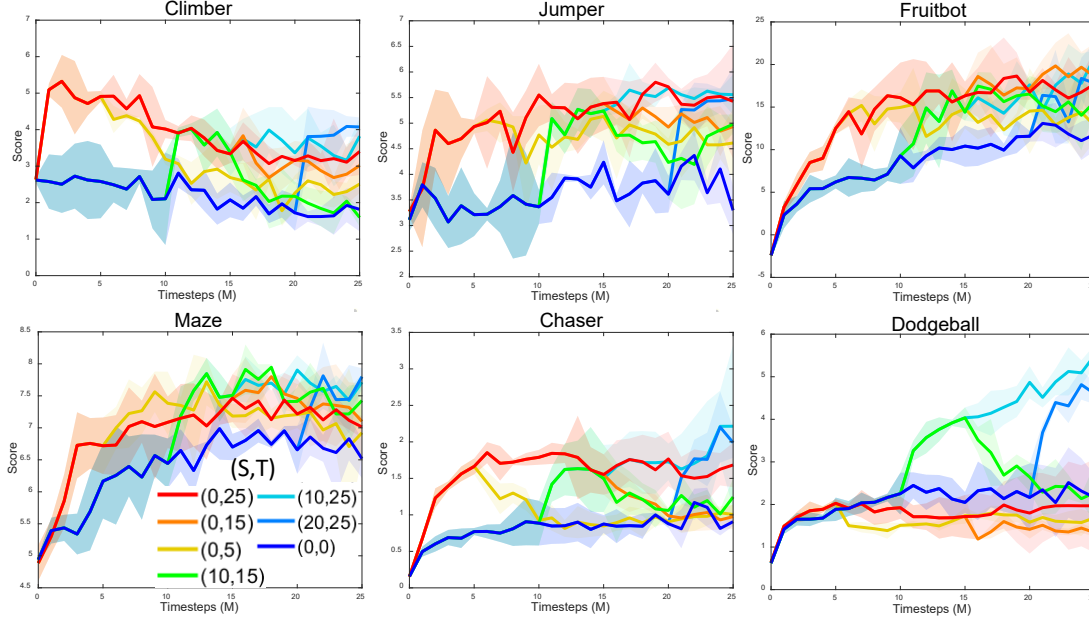


Figure 22. Comparison generalization on unseen backgrounds according to usage period of augmentation with InDA (*cutout color*): Chaser and Dodgeball have benefited from delayed augmentation because the early used *cutout color* ruins the training.

G. Benchmark on Modified Open AI Procgen

We compare the training and test performance on various environments with each augmentation. We also use DrAC (Raileanu et al., 2020), RAD (Laskin et al., 2020), Rand-FM (Lee et al., 2019) as baselines. In every results, we train the agent for 25M timesteps, except the ExDA. ExDA is trained with 0.5M after training 20M with PPO. We also compare the average score after normalized by PPO’s score and indicate the best score as bold except the Oracle. Red one is the Oracle score, which is trained on test environments such as *easybg-test*, *easy-test*. Mean and standard deviation is calculated after five runs (*random convolution*, *crop*) and three runs (*color jitter*, *cutout color*, *gray*). For your information, RAD does not work well when using crop, because we use (Raileanu et al., 2020)’s crop method which is different with (Laskin et al., 2020).

G.1. Random convolution

	Easy	PPO	DrAC	Rand_FM	RAD	InDA	ExDA
Climber		8.63	8.33	8.27	7.93	8.5	8.1
		± 0.462	± 0.407	± 0.187	± 0.37	± 0.291	± 0.268
Jumper		8.55	8.62	8.47	8.51	8.94	8.5
		± 0.168	± 0.075	± 0.13	± 0.102	± 0.09	± 0.183
Ninja		7.49	8.57	7.69	7.9	8.88	7.03
		± 0.421	± 0.069	± 0.529	± 0.652	± 0.343	± 0.058
Avg		1.00	1.04	0.99	0.99	1.07	0.96

Table 9. Training performance benchmark on *easy* with *random convolution*.

	Easy	PPO	DrAC	Rand_FM	RAD	InDA	ExDA
Climber		6.96	7.21	6.63	6.08	7.28	7.06
		± 0.651	± 0.447	± 0.39	± 0.264	± 0.341	± 0.541
Jumper		6.85	7.97	6.7	6.74	7.94	7.54
		± 0.192	± 0.128	± 0.167	± 0.299	± 0.185	± 0.158
Ninja		6.29	6.18	6.22	6.22	6.5	5.56
		± 0.529	± 0.193	± 0.57	± 0.324	± 0.191	± 0.158
Avg		1.00	1.06	0.97	0.95	1.08	1

Table 10. Test performance benchmark on unseen backgrounds (*easy*, *random convolution*).

Easybg	PPO	Oracle	DrAC	Rand-FM	RAD	InDA	ExDA
Climber	12.35	9.78	11.23	12.2	12.15	10.89	12.07
	± 0.083	± 0.306	± 0.353	± 0.128	± 0.09	± 0.162	± 0.073
Coinrun	9.64	7.11	9.17	9.57	9.56	8.81	9.44
	± 0.07	± 0.205	± 0.161	± 0.126	± 0.107	± 0.992	± 0.149
Fruitbot	29.78	29.74	26.07	30.19	29.92	26.17	28.76
	± 0.899	± 0.443	± 0.658	± 0.512	± 0.623	± 0.575	± 0.79
Heist	9	7.21	5.95	7.7	7.94	5.15	8.72
	± 0.513	± 0.27	± 0.343	± 0.6	± 0.919	± 0.614	± 0.533
Jumper	8.95	8.72	8.86	8.91	9.04	8.78	8.94
	± 0.066	± 0.119	± 0.088	± 0.13	± 0.135	± 0.172	± 0.048
Maze	9.75	8.56	8.1	9.61	9.51	9.12	9.73
	± 0.513	± 0.27	± 0.343	± 0.6	± 0.919	± 0.614	± 0.533
Ninja	9.75	7.81	9.43	9.75	9.78	9.53	9.7
	± 0.073	± 0.422	± 0.109	± 0.084	± 0.03	± 0.113	± 0.062
Avg	1.00	0.85	0.98	0.98	0.88	0.88	0.98

Table 11. Training performance benchmark on *easybg* with *random convolution*.

Easybg	PPO	Oracle	DrAC	Rand-FM	RAD	InDA	ExDA
Climber	1.97	9.78	7.13	2	2.34	7.36	8.11
	± 0.51	± 0.306	± 0.419	± 0.59	± 1.258	± 0.273	± 0.457
Coinrun	5.48	7.11	7.54	5.65	5.48	7.14	7.81
	± 0.583	± 0.205	± 0.188	± 0.216	± 0.542	± 0.479	± 0.388
Fruitbot	10.83	29.74	19.77	15.19	11.61	21.93	23.57
	± 1.908	± 0.443	± 0.77	± 3.363	± 4.615	± 0.664	± 0.745
Heist	5.18	7.21	5.47	5.03	4.78	4.96	8.15
	± 0.838	± 0.27	± 0.326	± 0.6	± 0.785	± 0.777	± 0.633
Jumper	3.38	8.72	8.14	4.12	3.77	8.16	7.87
	± 0.368	± 0.119	± 0.17	± 0.514	± 0.435	± 0.231	± 0.485
Maze	6.48	8.56	6.4	6.6	6.29	8.41	8.92
	± 0.523	± 0.665	± 0.419	± 0.494	± 0.466	± 0.436	± 0.155
Ninja	3.83	7.81	6.8	3.36	3.98	6.61	6.85
	± 0.462	± 0.422	± 0.243	± 0.505	± 0.44	± 0.327	± 0.25
Avg	1.00	2.33	1.86	1.08	1.04	1.92	2.11

Table 12. Test performance benchmark on unseen backgrounds (*easybg*, *random convolution*).

G.2. Crop

Easybg	PPO	DrAC	RAD	InDA	ExDA
Bigfish	14.08	15.92	5.05	19.35	11.07
	± 2.229	± 1.535	± 3.718	± 2.792	± 3.683
Chaser	5.63	3.97	1.24	6.52	4.81
	± 0.467	± 0.642	± 0.253	± 0.825	± 0.325
Dodgeball	7.71	10.74	1.23	12.74	6.74
	± 0.678	± 0.711	± 0.944	± 1.729	± 0.815
Heist	9	7.58	4.53	8.15	8.79
	± 0.513	± 0.11	± 0.266	± 0.57	± 0.424
Maze	9.75	9.03	3.95	9.63	9.72
	± 0.033	± 0.348	± 3.418	± 0.143	± 0.026
Plunder	7.18	10.73	0	10.29	6.59
	± 0.73	± 1	± 0	± 0.285	± 1.108
Avg	1.00	1.08	0.28	1.25	0.91

Table 13. Training performance benchmark on *easybg* with *crop*.

Easybg	PPO	DrAC	RAD	InDA	ExDA
Bigfish	7.43	13.63	4.93	15.19	6.35
	± 1.65	± 1.504	± 3.696	± 2.724	± 2.466
Chaser	4.83	3.59	1.2	5.86	4.48
	± 0.56	± 0.519	± 0.259	± 0.745	± 0.379
Dodgeball	3.78	9.26	1.11	11.92	3.79
	± 0.659	± 0.685	± 0.831	± 1.556	± 0.748
Heist	4.13	5.4	3.81	5.91	5.35
	± 0.146	± 0.448	± 0.412	± 0.516	± 0.22
Maze	6.79	7.77	3.9	8.01	7.74
	± 0.158	± 0.328	± 3.377	± 0.288	± 0.054
Plunder	5.94	9.49	0	8.98	5.98
	± 0.698	± 0.605	± 0	± 0.369	± 0.944
Avg	1.00	1.519	0.459	1.798	1.094

Table 14. Test performance benchmark on unseen levels (*easybg*, *crop*).

G.3. Color jitter

Easy	PPO	DrAC	RAD	InDA	ExDA
Climber	8.5	9.33	8.64	9.43	8.18
	± 0.575	± 0.212	± 0.156	± 0.21	± 0.45
Jumper	8.54	8.64	8.63	8.92	8.44
	± 0.22	± 0.135	± 0.17	± 0.174	± 0.185
Ninja	7.48	8.69	8.24	9.23	7.37
	± 0.324	± 0.331	± 0.251	± 0.081	± 0.212
Avg	1.00	1.09	1.04	1.13	0.98

Table 15. Training performance benchmark on *easy* with *color jitter*.

	Easy	PPO	DrAC	RAD	InDA	ExDA
Climber		6.92 ± 0.761	8.53 ± 0.422	8.37 ± 0.023	8.66 ± 0.24	8.14 ± 0.477
Jumper		6.89 ± 0.223	7.58 ± 0.053	7.86 ± 0.297	7.97 ± 0.292	7.25 ± 0.131
Ninja		6.39 ± 0.585	6.79 ± 0.32	7.31 ± 0.613	7.57 ± 0.555	6.2 ± 0.085
Avg		1.00	1.13	1.16	1.2	1.07

Table 16. Test performance benchmark on unseen backgrounds (*easy, color jitter*).

Easybg	PPO	Oracle	DrAC	RAD	InDA	ExDA
Climber	12.31 ± 0.092	9.85 ± 0.298	11.84 ± 0.223	12 ± 0.256	11.94 ± 0.071	12.04 ± 0.152
Coinrun	9.61 ± 0.074	7.2 ± 0.195	8.94 ± 0.285	8.62 ± 0.091	9.74 ± 0.05	9.45 ± 0.09
Fruitbot	30.2 ± 0.691	29.69 ± 0.619	30.05 ± 0.611	29.48 ± 0.507	26.87 ± 0.912	29 ± 0.878
Heist	8.82 ± 0.523	7.33 ± 0.308	7.22 ± 0.76	6.89 ± 0.348	7.63 ± 0.338	8.53 ± 0.307
Jumper	8.97 ± 0.075	8.67 ± 0.132	8.9 ± 0.05	8.94 ± 0.029	9.03 ± 0.123	9.03 ± 0.086
Maze	9.75 ± 0.035	8.08 ± 0.101	9.46 ± 0.404	9.46 ± 0.184	9.3 ± 0.379	9.67 ± 0.111
Ninja	9.74 ± 0.087	7.56 ± 0.286	9.52 ± 0.393	9.65 ± 0.112	9.75 ± 0.046	9.54 ± 0.171
Avg	1.00	0.85	0.95	0.94	0.96	0.98

Table 17. Training performance benchmark on *easybg* with *color jitter*.

Easybg	PPO	Oracle	DrAC	RAD	InDA	ExDA
Climber	1.82 ± 0.605	9.85 ± 0.298	5.05 ± 0.407	4.31 ± 0.492	4.25 ± 0.338	4.34 ± 0.856
Coinrun	5.42 ± 0.744	7.2 ± 0.195	6.46 ± 0.526	6.47 ± 0.194	7.13 ± 0.372	6.53 ± 0.375
Fruitbot	11.78 ± 1.949	29.69 ± 0.619	9.49 ± 8.098	8.51 ± 1.941	10.88 ± 2.263	18 ± 7.442
Heist	4.79 ± 0.323	7.33 ± 0.308	5.65 ± 0.984	5.39 ± 0.745	5.66 ± 0.271	5.43 ± 0.508
Jumper	3.3 ± 0.467	8.6 ± 0.132	5.65 ± 0.09	5.67 ± 0.953	5.81 ± 0.369	5.31 ± 0.351
Maze	6.52 ± 0.304	8.08 ± 0.101	8.22 ± 0.455	8.26 ± 0.175	8.35 ± 0.238	8.65 ± 0.017
Ninja	3.56 ± 0.363	7.56 ± 0.286	4.22 ± 0.487	4.18 ± 0.475	4.34 ± 0.345	4.07 ± 0.332
Avg	1.00	2.4	1.44	1.37	1.43	1.48

Table 18. Test performance benchmark on unseen backgrounds (*easybg, color jitter*).

G.4. Gray

Easybg	PPO	Oracle	DrAC	RAD	InDA	ExDA
Climber	12.31 ± 0.092	9.85 ± 0.298	11.12 ± 0.26	11.84 ± 0.505	11.9 ± 0.115	12.06 ± 0.03
Coinrun	9.61 ± 0.074	7.2 ± 0.195	9.53 ± 0.135	9.49 ± 0.188	9.74 ± 0.046	9.48 ± 0.08
Fruitbot	30.2 ± 0.691	29.69 ± 0.619	30.01 ± 0.572	29.6 ± 0.27	28.03 ± 0.994	29.32 ± 0.937
Heist	8.82 ± 0.523	7.33 ± 0.308	6.24 ± 0.214	6.53 ± 0.474	5.51 ± 0.146	8.51 ± 0.225
Jumper	8.54 ± 0.22	8.67 ± 0.132	8.91 ± 0.19	8.93 ± 0.247	9.18 ± 0.18	8.95 ± 0.075
Maze	9.75 ± 0.035	8.08 ± 0.101	9.46 ± 0.192	9.48 ± 0.08	9.2 ± 0.367	9.75 ± 0.087
Ninja	9.74 ± 0.087	7.56 ± 0.286	9.73 ± 0.045	9.61 ± 0.096	9.6 ± 0.081	9.72 ± 0.021
Avg	1	0.85	0.93	0.94	0.95	0.99

Table 19. Training performance benchmark on *easybg* with *gray*.

Easybg	PPO	Oracle	RAD	DrAC	InDA	ExDA
Climber	1.82 ± 0.605	9.85 ± 0.298	1.75 ± 0.654	1.81 ± 0.211	1.24 ± 0.502	2.45 ± 0.727
Coinrun	5.42 ± 0.744	7.2 ± 0.195	5.34 ± 0.751	5.31 ± 0.501	6.05 ± 0.465	5.79 ± 0.061
Fruitbot	11.78 ± 1.949	29.69 ± 0.619	17.57 ± 0.191	15.47 ± 1.449	15.12 ± 0.958	15.81 ± 0.11
Heist	4.79 ± 0.323	7.33 ± 0.308	5.43 ± 0.18	5.15 ± 0.172	4.32 ± 0.112	5.1 ± 0.504
Jumper	6.89 ± 0.223	8.67 ± 0.132	2.7 ± 0.894	4.07 ± 0.46	3.55 ± 0.992	4.47 ± 0.415
Maze	6.52 ± 0.304	8.08 ± 0.101	7.77 ± 0.611	7.93 ± 0.104	7.67 ± 0.312	8.33 ± 0.119
Ninja	3.56 ± 0.363	7.56 ± 0.286	3.72 ± 0.131	3.91 ± 0.62	4.02 ± 0.666	4.03 ± 0.071
Avg	1	2.2	1.03	1.04	0.97	1.13

Table 20. Test performance benchmark on unseen backgrounds (*easybg*, *gray*).

Easy	PPO	DrAC	RAD	InDA	ExDA
Climber	8.5 ± 0.575	6.95 ± 0.547	7.55 ± 0.256	7.22 ± 0.312	8.05 ± 0.461
Jumper	8.54 ± 0.22	8.4 ± 0.224	8.58 ± 0.199	8.85 ± 0.015	8.5 ± 0.224
Ninja	7.48 ± 0.324	6.67 ± 0.435	7.1 ± 0.718	8.91 ± 0.165	7.05 ± 0.24
Avg	1	0.9	0.95	1.026	0.96

Table 21. Training performance benchmark on *easybg* with *gray*.

	Easy	PPO	DrAC	RAD	InDA	ExDA
Climber		6.92 ± 0.761	4.49 ± 0.332	5.57 ± 0.307	5.11 ± 0.483	7.24 ± 0.721
Jumper		6.89 ± 0.223	5.38 ± 0.215	6.59 ± 0.055	6.35 ± 0.234	6.87 ± 0.182
Ninja		6.39 ± 0.585	5.67 ± 0.318	5.14 ± 0.628	6.84 ± 0.206	6.01 ± 0.651
Avg		1	0.77	0.86	0.91	0.99

Table 22. Test performance benchmark on unseen backgrounds (*easy*, *gray*).

G.5. Cutout color

Easybg	PPO	Oracle	DrAC	RAD	InDA	ExDA
Climber	12.31 ± 0.092	9.85 ± 0.298	11.92 ± 0.158	8.26 ± 0.663	11.76 ± 0.027	12.07 ± 0.127
Coinrun	9.61 ± 0.074	7.2 ± 0.195	9.23 ± 0.323	8.07 ± 0.645	9.7 ± 0.084	9.39 ± 0.012
Fruitbot	30.2 ± 0.691	29.69 ± 0.619	29.73 ± 0.898	29.2 ± 0.64	27.18 ± 1.302	28.95 ± 0.907
Heist	8.82 ± 0.523	7.33 ± 0.308	8.47 ± 0.397	6.25 ± 0.704	6.1 ± 0.693	8.65 ± 0.21
Jumper	8.97 ± 0.075	8.67 ± 0.132	8.87 ± 0.123	8.75 ± 0.131	9.1 ± 0.081	8.91 ± 0.053
Maze	9.75 ± 0.035	8.08 ± 0.101	9.41 ± 0.134	9.17 ± 0.118	9.27 ± 0.125	9.74 ± 0.133
Ninja	9.74 ± 0.087	7.56 ± 0.286	9.65 ± 0.138	7.17 ± 1.993	9.72 ± 0.02	9.7 ± 0.02
Bigfish	13.89 ± 3.127	13.22 ± 1.488	2.54 ± 0.13	5.19 ± 3.658	1.95 ± 0.311	11.22 ± 3.66
Chaser	5.49 ± 0.562	3.04 ± 0.183	2.88 ± 0.699	1.98 ± 0.112	3.34 ± 0.755	5 ± 0.187
Dodgeball	7.76 ± 0.859	5.74 ± 1.118	5.71 ± 1.008	5.98 ± 0.103	2.79 ± 1.612	6.57 ± 0.693
Plunder	7.15 ± 0.95	6.05 ± 0.58	5.43 ± 0.082	4.34 ± 0.24	4.92 ± 0.625	6.87 ± 1.255
Avg	1.00	0.82	0.82	0.72	0.76	0.94

Table 23. Training performance benchmark on *easybg* with *cutout color*.

Easy	PPO	Oracle	DrAC	RAD	InDA	ExDA
Climber	8.5 ± 0.575	9.85 ± 0.298	7.69 ± 0.237	6.67 ± 0.381	9.02 ± 0.473	8.02 ± 0.506
Jumper	7.48 ± 0.324	7.56 ± 0.286	6.28 ± 0.257	5.6 ± 0.276	8.57 ± 0.122	7.41 ± 0.125
Ninja	8.54 ± 0.22	8.67 ± 0.132	8.45 ± 0.183	8.32 ± 0.051	8.93 ± 0.166	8.53 ± 0.095
Avg	1.00	1.06	0.91	0.84	1.08	0.98

Table 24. Training performance benchmark on *easy* with *cutout color*.

Easybg	PPO	Oracle	DrAC	RAD	InDA	ExDA
Climber	1.82 ± 0.605	9.85 ± 0.298	3.54 ± 0.164	3.97 ± 0.999	3.4 ± 0.645	4.29 ± 0.154
Coinrun	5.42 ± 0.744	7.2 ± 0.195	5.87 ± 0.251	5.93 ± 0.061	6.2 ± 0.357	6.41 ± 0.131
Fruitbot	11.78 ± 1.949	29.69 ± 0.619	18.18 ± 3.744	19.24 ± 3.385	17.69 ± 4.026	17.7 ± 0.888
Heist	4.79 ± 0.323	7.33 ± 0.308	6.6 ± 0.092	5.76 ± 0.551	4.97 ± 0.33	7.51 ± 0.119
Jumper	3.3 ± 0.467	8.67 ± 0.132	4.99 ± 0.114	5.48 ± 0.28	5.43 ± 1.116	6.02 ± 0.235
Maze	6.52 ± 0.304	8.08 ± 0.101	7.33 ± 0.223	7.66 ± 0.243	7.01 ± 0.17	7.83 ± 0.22
Ninja	3.56 ± 0.363	7.56 ± 0.286	4.29 ± 0.245	3.96 ± 0.152	3.75 ± 0.333	3.76 ± 0.348
Bigfish	3.4 ± 0.487	13.22 ± 1.488	1.29 ± 0.08	2.5 ± 2.331	1.29 ± 0.152	4.49 ± 0.776
Chaser	0.91 ± 0.061	3.04 ± 0.183	1.08 ± 0.038	1.13 ± 0.157	1.68 ± 0.305	1.73 ± 0.698
Dodgeball	2.17 ± 0.53	5.74 ± 1.118	3.92 ± 0.53	4.02 ± 0.345	1.97 ± 1.098	4.37 ± 0.527
Plunder	6.87 ± 0.933	6.05 ± 0.58	5.27 ± 0.208	4.77 ± 0.612	4.71 ± 0.622	6.45 ± 1.232
Avg	1.00	2.51	1.27	1.33	1.19	1.53

Table 25. Test performance benchmark on unseen backgrounds (*easybg*, *cutout color*).

Easy	PPO	Oracle	DrAC	RAD	InDA	ExDA
Climber	6.92 ± 0.761	9.85 ± 0.298	6.54 ± 0.213	5.24 ± 0.417	7.61 ± 0.486	7.25 ± 0.325
Jumper	6.39 ± 0.585	7.56 ± 0.286	5.06 ± 0.137	4.9 ± 0.382	6.71 ± 0.352	5.78 ± 0.488
Ninja	6.89 ± 0.223	8.67 ± 0.132	6.88 ± 0.083	6.79 ± 0.278	6.81 ± 0.355	6.92 ± 0.212
Avg	1.00	1.29	0.91	0.84	1.05	0.99

Table 26. Test performance benchmark on unseen backgrounds (*easy*, *cutout color*).

Easybg	PPO	DrAC	RAD	InDA	ExDA
Climber	11.14 ± 0.077	10.77 ± 0.279	7.26 ± 0.843	9.45 ± 0.193	10.75 ± 0.114
Coinrun	8.64 ± 0.05	8.36 ± 0.348	6.89 ± 0.503	7.76 ± 0.096	8.32 ± 0.224
Fruitbot	28.26 ± 0.461	26.88 ± 1.276	26.22 ± 1.258	23.79 ± 0.971	26.33 ± 0.894
Heist	4.07 ± 0.07	3.92 ± 0.276	2.27 ± 0.448	2.15 ± 0.553	3.93 ± 0.184
Jumper	7.38 ± 0.15	7.32 ± 0.195	6.98 ± 0.199	6.68 ± 0.24	7.25 ± 0.117
Maze	6.8 ± 0.2	6.84 ± 0.137	6.04 ± 0.258	5.91 ± 0.03	6.17 ± 0.162
Ninja	8.56 ± 0.061	8.63 ± 0.132	6.28 ± 1.866	7.81 ± 0.21	8.34 ± 0.119
Bigfish	7.16 ± 2.263	0.91 ± 0.037	2.29 ± 2.306	0.95 ± 0.06	6.04 ± 2.783
Chaser	4.54 ± 0.503	2.61 ± 0.509	1.8 ± 0.12	2.47 ± 0.506	4.22 ± 0.331
Dodgeball	3.78 ± 0.823	2.71 ± 0.362	2.53 ± 0.135	1.26 ± 0.48	2.82 ± 0.593
Plunder	5.99 ± 0.814	5.08 ± 0.305	4.07 ± 0.479	4.55 ± 0.393	5.83 ± 1.061
Avg	1.00	0.83	0.69	0.69	0.93

Table 27. Test performance benchmark on unseen levels (*easybg*, *cutout color*).

Easy	PPO	DrAC	RAD	InDA	ExDA
Climber	5.45 ± 0.77	5.9 ± 0.352	5.3 ± 0.307	4.26 ± 0.122	5.71 ± 0.303
Jumper	5.81 ± 0.227	6.01 ± 0.389	4.93 ± 0.08	4.56 ± 0.161	5.43 ± 0.333
Ninja	5.77 ± 0.09	5.67 ± 0.023	5.8 ± 0.071	5.65 ± 0.166	5.87 ± 0.079
Avg	1.00	1.03	0.94	0.85	1

Table 28. Test performance benchmark on unseen levels (*easy*, *cutout color*).